Observations of Lower-Stratospheric $ClONO_2$, HNO_3, and Aerosol by the *UARS* CLAES Experiment between January 1992 and April 1993

A. E. ROCHE, J. B. KUMER, J. L. MERGENTHALER, R. W. NIGHTINGALE, W. G. UPLINGER, G. A. ELY, AND J. F. POTTER

Lockheed Palo Alto Research Laboratory, Palo Alto, California

D. J. WUEBBLES, P. S. CONNELL, AND D. E. KINNISON

Lawrence Livermore National Laboratory, Livermore, California

(Manuscript received 6 April 1994, in final form 14 July 1994)

ABSTRACT

This paper discusses simultaneous measurements of stratospheric $ClONO_2$, HNO_3, temperature, and aerosol extinction coefficient by the Cryogenic Limb Array Etalon Spectrometer (CLAES) on the NASA *Upper Atmosphere Research Satellite* (*UARS*), obtained over the period 9 January 1992 through 23 April 1993. The discussion concentrates on the stratosphere region near 21 km of particular interest to heterogeneously driven ozone depletion. For periods between 12 June and 1 September 1992 at latitudes poleward of about 60°S, when temperatures were below type I polar stratospheric cloud (PSC) formation thresholds throughout the lower stratosphere, CLAES observed high levels of PSCs coincident with highly depleted fields of both HNO_3 and $ClONO_2$. By 17 September, the incidence of PSCs had greatly diminished in the lower stratosphere, but both $ClONO_2$ and HNO_3 remained highly depleted. These observations are consistent with the removal of gaseous HNO_3 through the formation of nitric acid trihydrate (NAT) particles and the removal of $ClONO_2$ through heterogeneous reactions on the particle surfaces. They also suggest substantial denitrification of the lower Antarctic vortex through sedimentation of PSC particles. In the Northern Hemisphere winter of 1992/93 far fewer PSCs were observed in the Arctic lower-stratosphere vortex, which had shorter periods and more localized regions of cold temperatures. Both HNO_3 and $ClONO_2$ maintained much higher levels inside the Arctic vortex than those seen in the Antarctic throughout the winter/spring period. Following 28 February 1993 when Arctic vortex temperatures rose above 195 K, $ClONO_2$ was observed in large quantities [>2.1 ppbv near 21 km] inside the vortex. The persistence of relatively high levels of HNO_3 inside the Arctic spring vortex compared with the low levels seen in the Antarctic spring vortex suggest a much lower level of denitrification in the Arctic.

1. Introduction

Chlorine nitrate ($ClONO_2$), nitric acid (HNO_3), and polar stratospheric clouds (PSCs) play key roles in the extensive depletion of ozone in the lower stratosphere over Antarctica each austral spring. Under the very cold conditions inside the South Polar winter vortex, HNO_3 is sequestered in PSCs mainly in the form of nitric acid trihydrate (NAT) particles. During the polar night, these clouds provide surfaces for the heterogeneous conversion of inactive chlorine in the reservoirs $ClONO_2$ and HCl to active chlorine. With the return of spring sunlight, active chlorine forms chlorine monoxide (ClO), which then proceeds through a series of catalytic reactions to destroy ozone (Solomon 1990). Such processes can also occur in the Arctic winter/spring stratosphere (Kawa et al. 1992a; Webster et al. 1993), although with much smaller associated ozone loss in the spring (Salawitch et al. 1993).

A large part of the current understanding of polar ozone processes has come from a series of airborne campaigns, particularly from the Airborne Antarctic Ozone Experiment (AAOE) in 1987 (Tuck et al. 1989), the Airborne Arctic Stratosphere Expedition (AASE1) in 1989 (Turco et al. 1990), and the AASE2 in 1991/92 (Rodriguez et al. 1993). The *Upper Atmosphere Research Satellite* (*UARS*), which was launched in 1991, builds on these measurements by providing global coverage of a range of stratospheric constituents over an extended period of time (Reber 1993). This paper discusses simultaneous measurements of stratospheric $ClONO_2$, HNO_3, temperature, and aerosol extinction coefficient by the Cryogenic Limb Array Etalon Spectrometer (CLAES) on the *UARS*, obtained over the period 9 January 1992 through 23 April 1993. CLAES observations of $ClONO_2$, HNO_3, and PSCs for selected days in the 1992 Antarctic winter have been published previously

Corresponding author address: Dr. A. E. Roche, Dept. 91/20, Bldg. 255, Lockheed Palo Alto Research Laboratory, 3251 Hanover Street, Palo Alto, CA 94304.

(Roche et al. 1993a; Mergenthaler et al. 1993). The present paper is intended to provide an overview of the observed morphological and seasonal behavior of these constituents in both hemispheres over a much longer period of time. The discussion concentrates on the high-latitude, lower-stratosphere region of prime interest to heterogeneously driven ozone depletion. With alternating coverage to 80° north and south latitudes, and a time span that includes two Northern and one Southern Hemisphere winter/spring period, we can observe seasonal and interhemispheric differences for the $ClONO_2$, HNO_3, and PSC fields in the vicinities of the polar vortices and examine the correlation of these differences with meteorological conditions.

2. General morphology of lower-stratospheric $ClONO_2$, HNO_3, and aerosol: January 1992 to April 1993

a. *Observational data*

CLAES derives geophysical quantities from the measurement of infrared spectral radiance emissions in a limb-viewing mode. Details of the instrument design are given in Roche et al. (1993b), and summary discussions of the spectroscopy involved in the retrieval of HNO_3 and $ClONO_2$, as well as the data quality associated with Version 5 data processing software, are given in Roche et al. (1993a). The present paper uses CLAES data processed with improved retrieval algorithms (data Versions 6 and 7), which has resulted in some reduction in the systematic error estimates listed in Roche et al. (1993a). The systematic and random (i.e., repeatability) errors for the data presented here are, for the HNO_3 volume mixing ratio (VMR), 20% and 1 part per billion by volume (ppbv), respectively, and for the $ClONO_2$ VMR, 30% and 0.3 ppbv, respectively. These are one-sigma, single-profile estimates and apply to the range 18 to 30 km, which is of most interest for this paper. Retrieval of aerosol extinction coefficients from CLAES radiance measurements is discussed in Mergenthaler et al. (1993). We estimate the systematic error in the majority of the aerosol extinction data used here (which is derived from the 790 cm^{-1} spectral channel) to be 20%, with a repeatability of 15% in the 18- to 25-km range. For PSCs, however, significantly larger errors can occur in the absolute values of the retrieved extinction coefficients during the coldest southern polar winter conditions, when particularly dense clouds are encountered. The PSC data presented for these periods is most useful, and is so used in this paper, for the study of morphological and seasonal behavior, rather than for detailed quantitative analysis. CLAES temperature is also used in this paper, for which we estimate a systematic error between 2 and 4 K, with the larger number associated primarily with very cold temperature conditions in the South Polar winter stratosphere. Temperature repeatability is estimated at 1–2 K. Finally, we estimate the systematic and random errors for the high-latitude CLAES CH_4 VMR used in this paper to be 20% and 0.1 ppmv, respectively. Retrieval of CH_4 VMR from CLAES radiance data is discussed in Kumer et al. (1993).

The potential vorticity (PV) data used in this paper were provided to us by G. Manney and coworkers at the Jet Propulsion Laboratory, who derive the quantities from National Meteorological Center (NMC) data (Manney and Zurek 1993).

CLAES acquires altitude profiles of constituents on 65-s centers and samples each latitude circle 30 times per day in a latitude band from either 34°S to 80°N or 34°N to 80°S, depending on the flight direction of *UARS*. The spacecraft is yawed 180 degrees approximately every 36 days, and the resulting geographical and temporal coverages of the CLAES data acquisition between 9 January 1992 and 23 April 1993 are shown in Fig. 1 for aerosol extinction coefficient and temperature, in Fig. 2 for $ClONO_2$ in comparison with the Lawrence Livermore National Laboratory (LLNL) 2D model, and in Fig. 3 for HNO_3 in comparison with the LLNL model. For reference purposes the *UARS* day numbers are given for every 10th day, where 9 January 1992 is *UARS* day 120, and 23 April 1993 is *UARS* day 590. The figures display the CLAES fields as daily zonal-mean values at 46 mb (near 21 km). The approximate 5-day data gaps at the yaw boundaries result from the operational requirement that the CLAES telescope door be closed several days prior to and following the yaw to guard against solar heat load to the stored cryogen via the telescope baffles and optics. The alternating viewing geometry and the data gap straddling the yaw mean that the closest interhemispheric comparisons between the fields for latitudes poleward of 34°N and 34°S are necessarily separated by about 5 days. For the majority of times and latitudes, however, this is a short enough period to preclude any major meteorological changes, allowing for reasonable comparisons across the gap. The good consistency of the displayed fields across the 5-day gaps for the latitude overlap band 34°N to 34°S also lends confidence to the "continuity" of the behavior of the mapped fields for periods immediately prior to and following the yaw data interrupt segments.

b. *Pinatubo sulfate aerosol and polar stratospheric clouds*

Figure 1a shows both the evolution of the Pinatubo sulfate aerosol layer over the 16-month period and the occurrence of polar stratospheric clouds in the Southern Hemisphere winter. The Pinatubo layer with its peak values still observed between about 30°N and 30°S in early January 1992 dissipated throughout the 16-month period at 46 mb, with extinction values in April 1993 having dropped by a factor 3 to 4 in the Tropics and 2

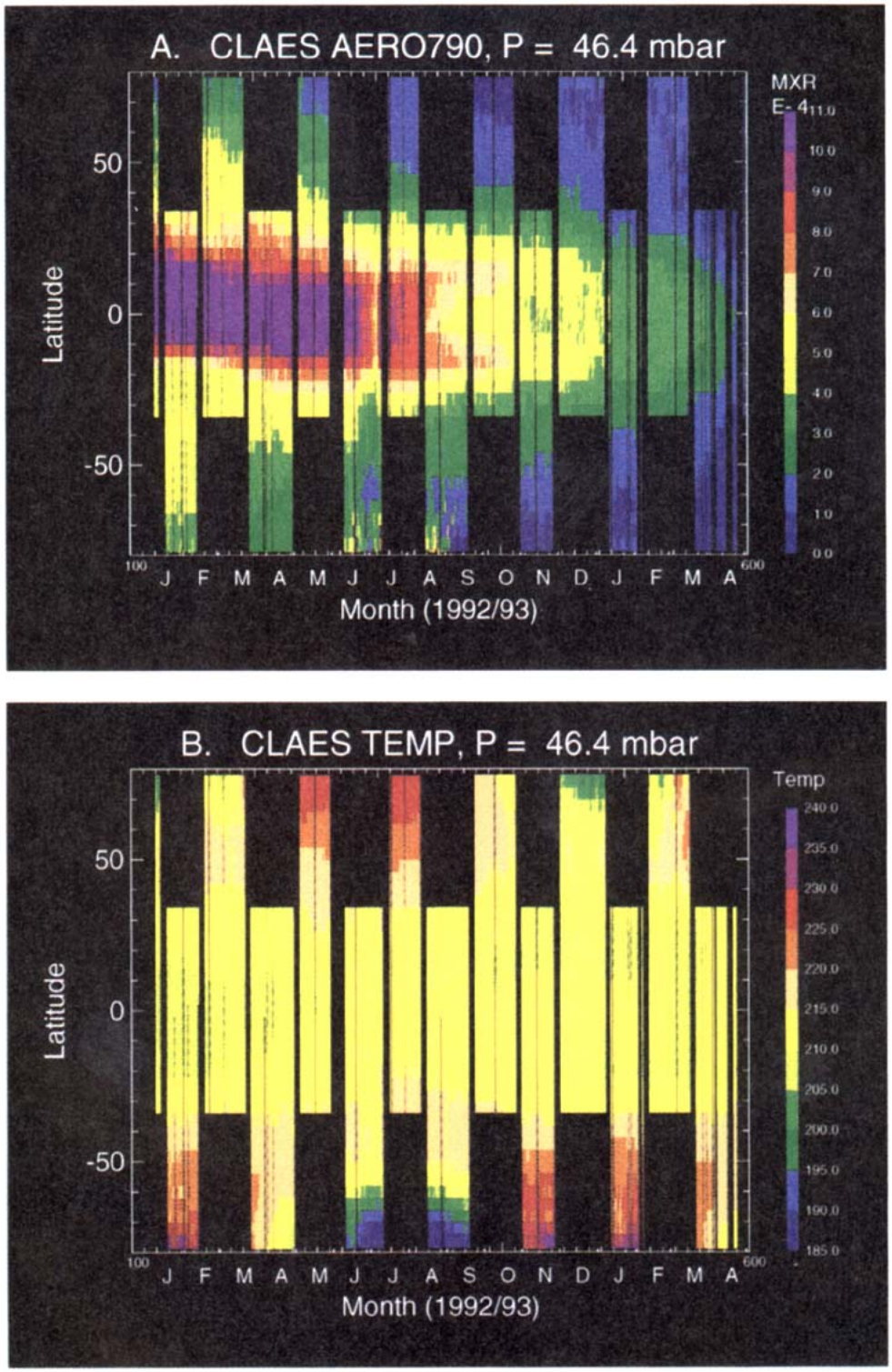

FIG. 1. (a) Zonal-mean aerosol extinction coefficients near 21 km (in units of 10^{-4} km^{-1}). (b) Temperature (K) as observed by CLAES between 9 January 1992 and 23 April 1993. The CLAES data are gridded in intervals of 1 day and 4° of latitude.

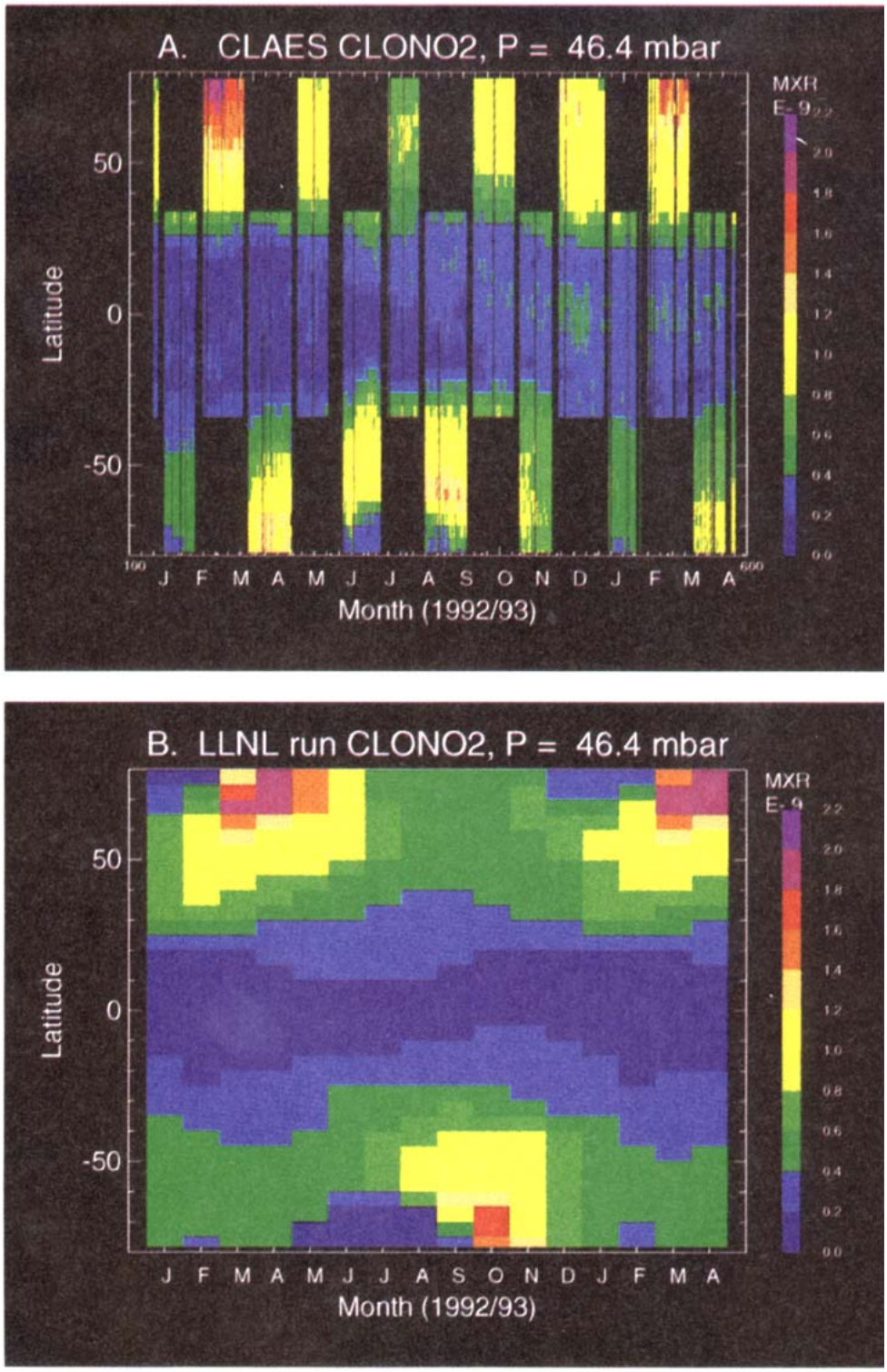

FIG. 2. (a) Zonal-mean volume mixing ratio for $ClONO_2$ (ppbv) as observed by CLAES between 9 January 1992 and 23 April 1993. (b) Zonal-mean VMR for $ClONO_2$ as calculated by the LLNL 2D model for the same period. The CLAES data are gridded in intervals of 1 day and 4° of latitude; the model has intervals of 1 month and 5° of latitude.

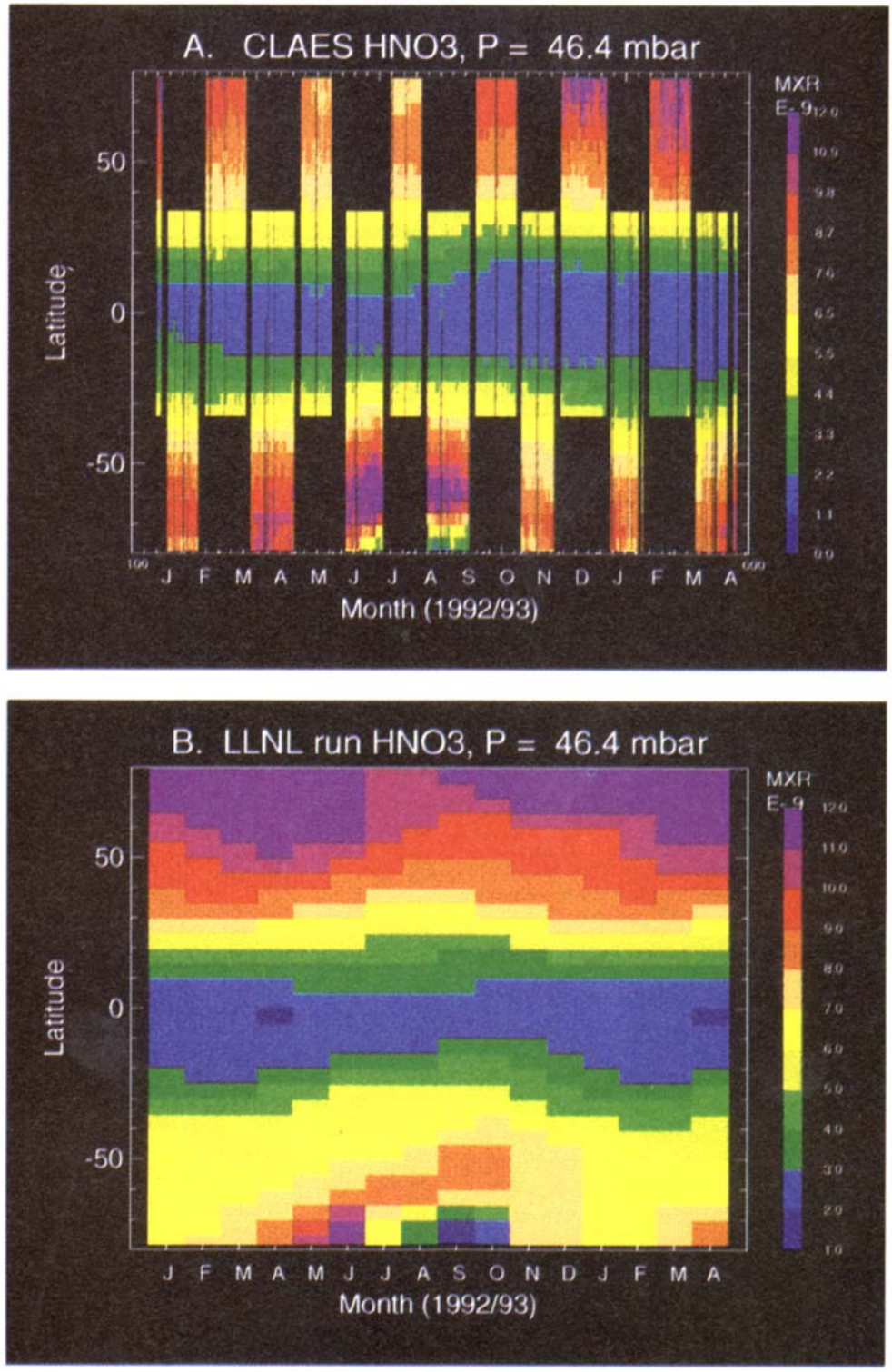

FIG. 3. (a) Zonal-mean volume mixing ratio for HNO_3 (ppbv) as observed by CLAES between 9 January 1992 and 23 April 1993. (b) Zonal-mean VMR for HNO_3 as calculated by the LLNL 2D model for the same period. The CLAES data are gridded in intervals of 1 day and 4° of latitude; the model has intervals of 1 month and 5° of latitude.

to 3 at higher latitudes in both hemispheres. However, in the observed periods in the Southern Hemisphere in June, July, and August 1992, high levels of extinction occur, mainly at latitudes poleward of 65°S. Examination of the observed temperatures for this period show them to be at least 5 K cooler than the 195-K approximate threshold value below which type I PSCs can begin to form. Type I PSCs in the Antarctic are expected to be mainly NAT (Hanson and Mauersberger 1988; Fahey et al. 1989; Marti and Mauersberger 1991), which is consistent with the observation of depleted HNO_3 in the same region, as can be seen in Fig. 3. Figure 1a is most useful for providing an overall picture of the temporal evolution of the global aerosol fields, but PSCs in particular can be highly structured spatially, and a zonal-mean representation of them conveys a limited amount of information. The fact that PSCs show up in this zonal-mean plot at the levels they do is an indication of their spatial extent, density, and persistence of occurrence in the South Polar winter. PSCs have also been observed by CLAES in the Northern Hemisphere winters but in a spatially more isolated form, and for shorter periods of time, reflecting the generally warmer vortex temperatures and shorter periods significantly below 195 K. These North Polar winter PSCs are not present in sufficient densities to appear in the Fig. 1a zonal-mean plot but are shown and discussed in section 4 as they appear in latitude/longitude cross sections.

c. $ClONO_2$ and HNO_3

Figure 2a illustrates the main morphological and seasonal features of the $ClONO_2$ fields as observed by CLAES at 46 mb, including the distinct interhemispheric difference between the winter poles associated with heterogeneous processing. The random error associated with these zonal-mean fields reduces to at least 0.1 ppbv compared with the 0.3-ppbv single-profile estimate listed above. The main features in Fig. 2a are seen to be low (<0.3 ppbv) and relatively constant VMR between about 25°N and 25°S and increasing VMR toward higher latitudes in both hemispheres, but significantly higher values near the winter/spring poles. For example, winter/spring Arctic values (mid-February through mid-March 1992, and again in February–March 1993) reach levels between 1.5 and 2 ppbv, whereas the summer Antarctic values in both years in February are less than 0.5 ppbv. The bias toward the winter pole is also evident for the Southern Hemisphere winter versus the Northern Hemisphere summer, with some notable differences. Early July 1992 Southern Hemisphere values from about 40° to 60°S are higher than the equivalent latitudinal range in the north. From about 65°S to the pole, however, very low values are seen, coincident with the observations of PSCs and low temperatures in Fig. 1, which implies that the depletion of $ClONO_2$ poleward of 65°S is due to heterogeneous processing on these PSC surfaces. Hemispheric differences with respect to heterogeneous processing are discussed in more detail in section 2. VMRs for the two southern summers (January 1992, January 1993) are lower than those for the July 1992 northern summer. This may result from the combination of interhemispheric dynamical differences and the steep gradient of $ClONO_2$ in the lower stratosphere, forcing observable differences when looking at the gas at this one (46 mb) pressure surface. Another aspect of the CLAES $ClONO_2$ fields shown in Fig. 2a is the small increase in equatorial values roughly time correlated with the decrease in aerosol extinction coefficient. A more detailed analysis will be required to establish whether this apparent change is related to aerosol-driven surface chemistry or dynamical effects such as aerosol-driven circulation changes or seasonal oscillations.

The Lawrence Livermore National Laboratory two-dimensional (2D) model is shown in Fig. 2b for comparison with the CLAES $ClONO_2$ data. This model has been described in Wuebbles et al. (1991) and Patten et al. (1994). It is a diurnally averaged 2D chemical–radiative–transport (CRT) model that currently determines the atmospheric distributions of 47 chemically active atmospheric trace constituents in the troposphere and stratosphere. It extends from pole to pole and from the surface to 60 km, with 5° latitude resolution and approximately 1.5-km vertical resolution. Activation of inorganic chlorine from HCl and $ClONO_2$ in the polar winter/spring stratosphere is accomplished in the model by representing the heterogeneous reactions of 1) HCl with $ClONO_2$ and HOCl both releasing Cl_2, which takes place predominantly on type I PSCs, and 2) the hydrolysis of $ClONO_2$ to release HOCl, which is faster on type II (water ice) particles. Heterogeneous reaction rate constants are based on empirical observations of Cl processing rates in the presence of PSCs, relative gas/surface reaction probabilities from laboratory results, and climatological fields of PSC occurrence frequency from satellite observations. Hydrolysis of N_2O_5 on PSCs is also represented. A microphysical treatment of PSCs is not incorporated into the current model, but the working assumption that all available HNO_3 and HCl are quickly incorporated into PSCs when present should be reasonably accurate. A proper treatment of the sedimentation of the larger particles (typically type II) also requires knowledge of the microphysical parameters (e.g., size distribution). In the current formulation HNO_3 is removed from the model at a rate grossly representing the time for a particle a few microns in size to fall several kilometers, during times when the climatological temperature falls below the type II formation threshold. This may overestimate actual dehydration/denitrification rates because model HNO_3 lost in this manner is completely removed without reappearing by evaporation at lower altitudes.

The hydrolysis of N_2O_5 and $ClONO_2$ on sulfate aerosols in the stratosphere is also included in the model, based on a time-dependent satellite-derived surface area density climatology for the 1992/93 period, gas/surface collision rates from kinetic theory, and laboratory reaction probabilities. The effect of temperature on the liquid sulfate aerosol composition is included in calculating the $ClONO_2$ reaction probability. The possibility of the presence of frozen sulfate aerosol particles, which may be more chemically active, is not included in the current model.

The model captures the primary morphological and seasonal features of the data—that is, low tropical $ClONO_2$ VMRs, the general buildup to high values in the polar winter/springs versus the polar summers, and the development of a deep depletion region poleward of 60°S in the southern winter/spring. The model gives noticeably lower values than the data for high latitudes in the autumn periods in the south (March–April 1992 and 1993) and the north (September–October 1992), possibly due to a weaker modeled downward circulation than that actually occurring for $ClONO_2$ during these periods. The model does not show any apparent increase with time of equatorial $ClONO_2$ at this pressure surface.

Figure 3a shows the HNO_3 VMR over the 15-month period on a 46-mb surface. The random error for these zonal-mean HNO_3 fields is estimated to be less than 0.4 ppbv. The overall morphological and seasonal behavior seen here has been observed previously by the Limb Infrared Monitor of the Stratosphere (LIMS) instrument for latitudes 64°S to 84°N and for the period October 1978 through May 1979 (Gille et al. 1984). CLAES extends these measurements to 80°S and includes a South Polar winter. These lower-stratospheric HNO_3 fields are characterized by low, and essentially invariant, VMR levels between 30°S and 30°N, and increasing values toward the poles. As was the case for $ClONO_2$, levels are typically higher near the winter poles. This is particularly evident in Fig. 3a when comparing the south winter polar region in early July and August with the same period for the north summer polar region, and in contrasting the 1993 northern winter months with the 1993 South Pole summer months. As with $ClONO_2$, greatly depleted HNO_3 values are seen at high latitudes in the South Pole winter especially in August, compared with the same region for the northern winter. These levels recover to more "climatological" values by the next southern look in November. As stated earlier, the depletion of high-latitude HNO_3 in the austral winter spring is consistent with the formation of type I PSCs at low temperatures.

The 2D model (Fig. 3b) captures the major morphological and seasonal features of the data, including the high-latitude depletion zone in the Southern Hemisphere winter. The most noticeable difference is the higher values near the North Pole in winter/spring 1992 in the model compared with the observations. The biggest difference is for March 1992, where the data indicate daily averages of about 8 ppbv versus a model monthly value in excess of 12 ppbv. The CLAES value is in reasonable agreement with balloon measurements for the same day and latitude (von Clarmann et al. 1993) and is also closer to the LIMS data (for 1979), suggesting that the model is overestimating the amount of HNO_3 for this period. The trends in the model and data, however, are similar for the period from February to July 1992. For example, the CLAES observations show a nearly linear decrease in HNO_3 VMR between February and July of 2.5 ppbv, or about 25%, while the model (not discernible for the color contours used in Fig. 3b, which are designed to emphasize lower values) shows a decrease also of about 2.5 ppbv, or about 20%. The CLAES data and model come back into much better quantitative agreement in the 1992/93 northern winter period. For example, in the February–March 1993 period the agreement is within 1 ppbv or about 12%. For the Southern Hemisphere the high-latitude agreement between the data and models is quite good, both in the seasonal evolution of the fields and in the absolute values.

Figures 4 and 5 provide a more quantitative look at the behavior of the $ClONO_2$ and HNO_3 fields in the lower Antarctic stratosphere in comparison with temperature and PSC activity. Figure 4a shows the temperature regimes for the 46-mb surface between 72 and 80°S for the south-looking days over the 15-month period, overlaid with aerosol extinction coefficient. Also included is NMC temperature to show the progression with respect to the type I PSC formation temperature for the gaps when CLAES was looking north. During the early periods (through April 1992) when the zonal-mean temperature was above 205 K, extinction coefficients are of the order of $(2–4) \times 10^{-4}$ km^{-1} and appear to be dropping slightly. At the beginning of the next southern look (12 June 1992) the NMC temperature has dropped to 193 K and reaches 185 K by 12 July. Large increases in extinction coefficient are seen during this period, indicating the development of PSCs. At the beginning of the 16 August southern look when the temperature was near 185 K (and had been this low from 16 July, as shown by the NMC data), high extinction values are still observed, showing the continued presence of PSCs. Toward the end of August these high extinction values abruptly drop off to levels lower than those seen in April 1992, this transition occurring while the temperature, as indicated by the NMC data, was close to 193 K. By the end of the September south-looking period and for the remaining south-looking periods between 2 November 1992 and 23 April 1993, the temperature remained in excess of 212 K and extinction coefficients remained low. We have calculated the approximate NAT sublimation temperature for the June–September 1992 period based on a formula of Hanson and Mauersberger (1988). Near the beginning of the period (15 June) CLAES measured 8 ppbv of

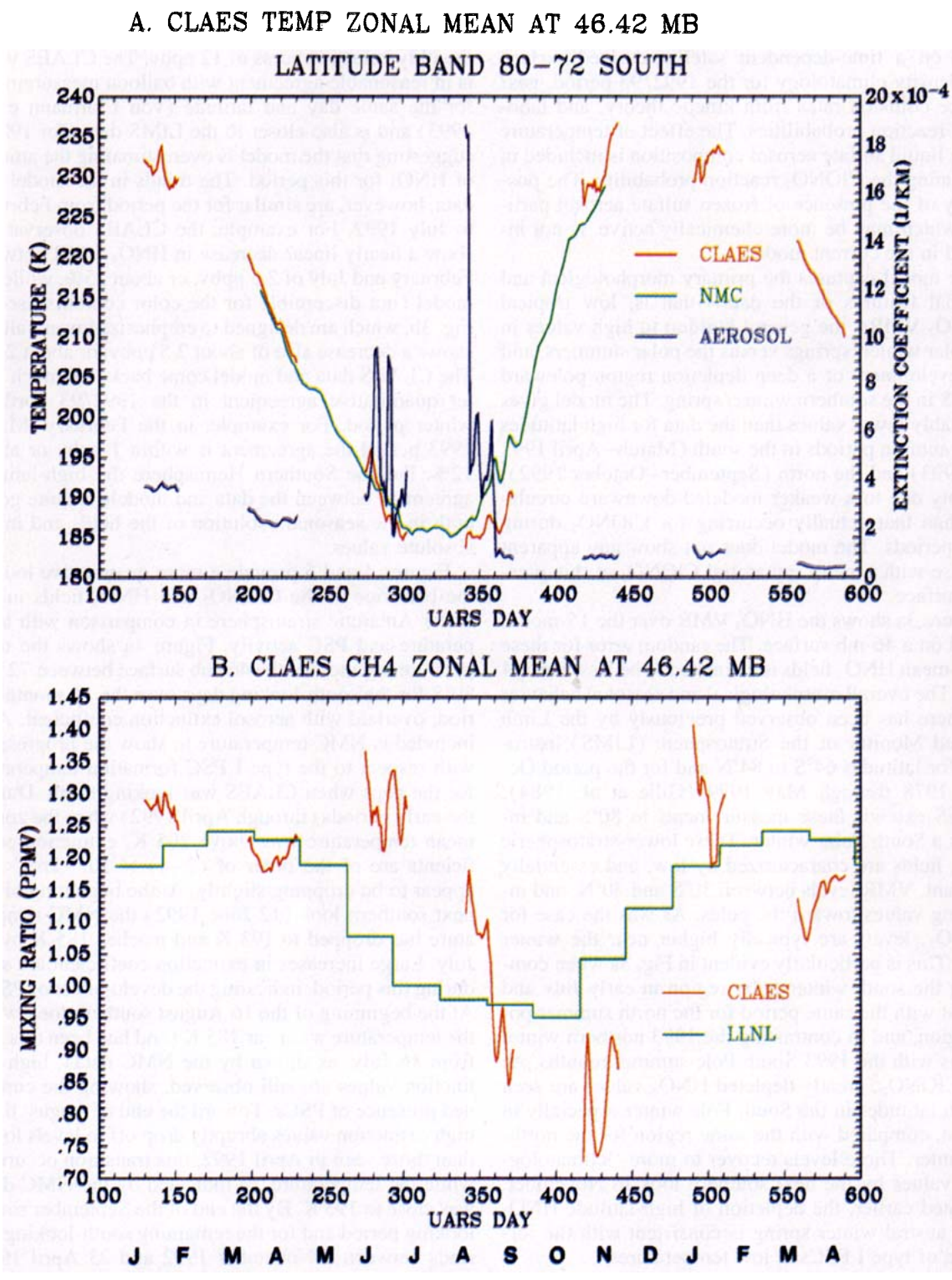

FIG. 4. (a) Line plots of the 72° to 80°S average value of zonal-mean CLAES temperature, NMC temperature, and CLAES aerosol extinction coefficient, for south-looking periods between 9 January 1992 and 23 April 1993. (b) Line plot of CLAES CH_4 VMR for the same period with LLNL model overlay. CLAES data have been averaged over 3-day intervals.

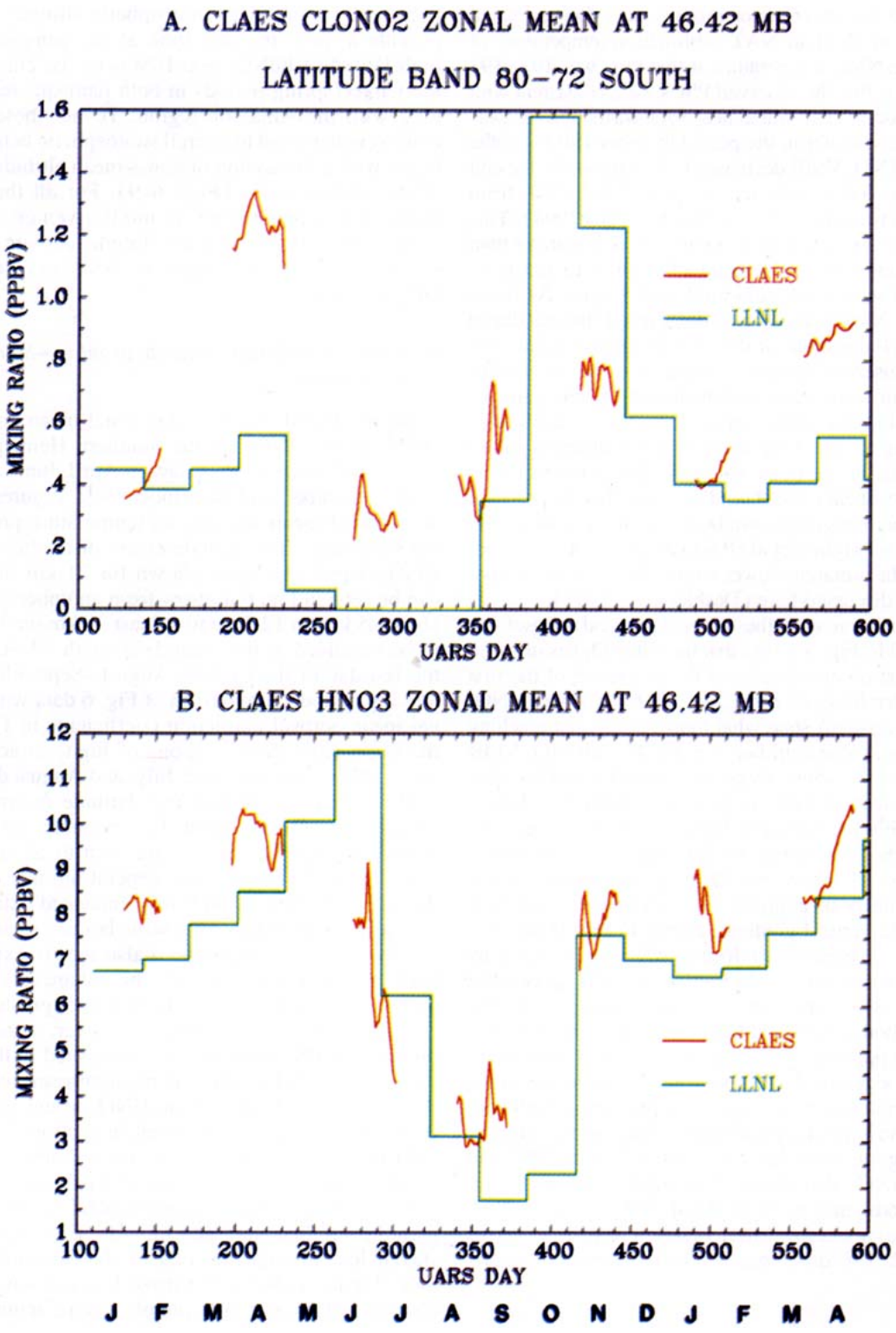

FIG. 5. (a) Line plot of the 72° to 80°S average value of the zonal-mean $ClONO_2$ VMR at 46 mb as observed by CLAES for south-looking periods between 9 January 1992 (*UARS* day 120) and 23 April 1993 (*UARS* day 590). Calculations from the LLNL 2D model are shown in overlay. (b) Same as (a) but for CLAES HNO_3 and LLNL model HNO_3. The CLAES data have been averaged over 3-day intervals.

HNO_3, and the water vapor mixing ratio was estimated at 4 ppmv to yield an NAT sublimation temperature of 194 K. The NMC temperature at that time was 192–193 K, indicating that the observed PSCs were consistent with NAT formation. The calculated NAT formation temperature decreased later in the period to about 190 K, as the CLAES–HNO_3 VMR decreased to 3–4 ppbv (by the end of August), and we inferred ~2 ppmv H_2O VMR from the balloon frost-point data of Deshler et al. (1994). This 190-K NAT formation temperature was still warmer than the NMC temperatures, which had dropped to 185 K by 9 July and stayed this cold until mid-August. As noted above, the NMC temperature did exceed the calculated 190-K NAT threshold at the end of August, coincident with the observed abrupt decrease in extinction coefficients at this same time. Sedimentation of PSC particles to lower altitudes (Fahey et al. 1990) is probably also contributing to the observation of low extinction values in the spring at the fixed 46-mb surface relevant to the Fig. 4a aerosol data. We should also note that the presence of sulfate aerosols may complicate the discussion of PSC composition (Molina et al. 1993) and their observed behavior in the Antarctic lower stratosphere during the period being discussed here (Deshler et al. 1994).

In comparison with the temperature and aerosol extinction fields, Fig. 5 shows that the $ClONO_2$ has dropped to its lowest observed value at the beginning of the first south winter look, in early June 1992, whereas HNO_3 appears to drop off somewhat more slowly, not reaching its minimum value until late August. The $ClONO_2$ VMR also appears to show recovery somewhat earlier than HNO_3. Both constituents in general maintain their lowest values during the period of highest PSC occurrence. As shown in the next section in discussing zonal-mean altitude profiles of HNO_3 and $ClONO_2$, the 46-mb surface is below the peak altitudes for both species, and both show strong vertical gradients above 46 mb. Descent of higher stratospheric air to 46 mb, which is indicated by the steep drop-off in the 46-mb CLAES CH_4 tracer data (Fig. 4b), would therefore be expected to increase the VMRs of both HNO_3 and $ClONO_2$ in the winter period. This is the opposite of what is observed and strengthens the case for removal of these constituents in the lower stratosphere through heterogeneous processes. Both constituents show good repeatability in their austral summer VMRs in going from January 1992 to January 1993, but whereas HNO_3 also shows close agreement for the autumn periods, that is, from April 1992 to April 1993, $ClONO_2$ has noticeably lower values in April 1993 versus April 1992. This difference will be the subject of further analysis.

3. High-latitude observations of HNO_3, $ClONO_2$, and aerosol in the Southern Hemisphere winter/spring

Figures 1–4 serve to illustrate the long-term zonal-mean seasonal morphology of the $ClONO_2$ and HNO_3 fields at a single lower-stratospheric altitude. We now provide a more detailed look at the behavior of the high-latitude $ClONO_2$ and HNO_3 fields, emphasizing the winter/spring periods in both hemispheres, beginning with the Antarctic region. To put these data in context with regard to overall stratospheric behavior we begin with a discussion of zonal-mean altitude profiles of the various fields (Figs. 6–9). For all the data in these figures, pressure (p) in mb is given on the right-hand scale, and approximate altitude, derived from the pressure as $Z^* = (3 - \log p) \times 16$ km, is given on the left-hand scale.

a. HNO_3: Zonal-mean altitude profiles—Southern Hemisphere

Figures 6 and 7 show 1-day zonal-mean profiles for HNO_3 and $ClONO_2$ for the Southern Hemisphere for six specific south-looking days in April, June, July, August, September, and November 1992. Figures 8 and 9 show zonal-mean aerosol and temperature profiles for the same days. The altitude extent of the high-latitude HNO_3 depletion region, shown for 21 km in Fig. 3a, can be seen in Fig. 6 to grow from an upper altitude of about 25 km on 12 June to at least 30 km on 9 July and to be sustained at this altitude through 17 September, the last day of the CLAES August–September south-looking period. Comparison of Fig. 6 data with the zonal-mean aerosol extinction coefficients in Fig. 8 for the same days shows regions of high extinction values—PSCs—for the June, July, and August days, typically within the altitude and latitude regime of the strongest HNO_3 depletion. For example, on 12 June enhanced extinction values are seen to about 26 km, from 75° to 80°S, the same general altitude extent of the HNO_3 depletion. On 9 July enhanced extinction is seen as high as 30 km in the same latitude region, while the deepest HNO_3 depletion is also seen to extend to at least 30 km. On 17 August, the enhanced extinction region still roughly defines the region of greatest HNO_3 depletion. By 17 September, however, although the presence of PSCs has greatly diminished in the vortex above about 18 km, there is no significant increase in the zonal-mean high-latitude HNO_3 at any altitude in the range shown. As discussed in section 2c, a sharp reduction in PSC activity at 46 mb was observed in late August coincident with the zonal-mean vortex temperature rising above the estimated NAT formation temperature for that time and altitude. Extinction values stayed low through the end of the September south look. Figure 8 shows that these low extinction values observed at 46 mb in September were actually characteristic of the vortex for all altitudes above about 18 km. From the section 2c discussion and the zonal-mean temperatures shown in Fig. 9 we might assume that PSC activity had essentially ceased throughout the vortex by 17 September, at least above 18 km, because temperatures were too warm for their existence. The

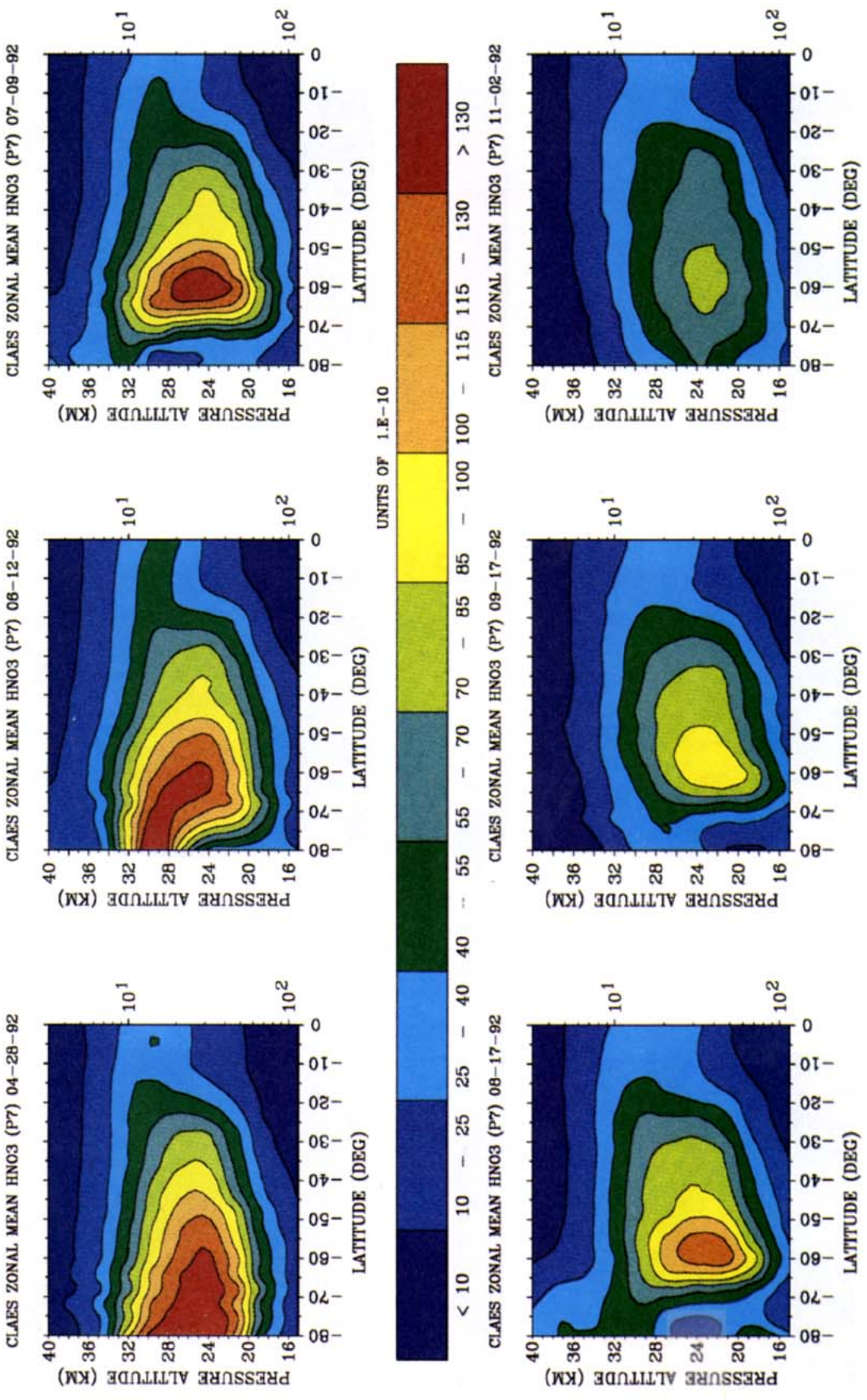

FIG. 6. Zonal-mean stratospheric altitude profiles of Southern Hemispheric HNO_3 VMR (ppbv $\times$ 10) as measured by CLAES for individual days in April, June, July, August, September, and November 1992.

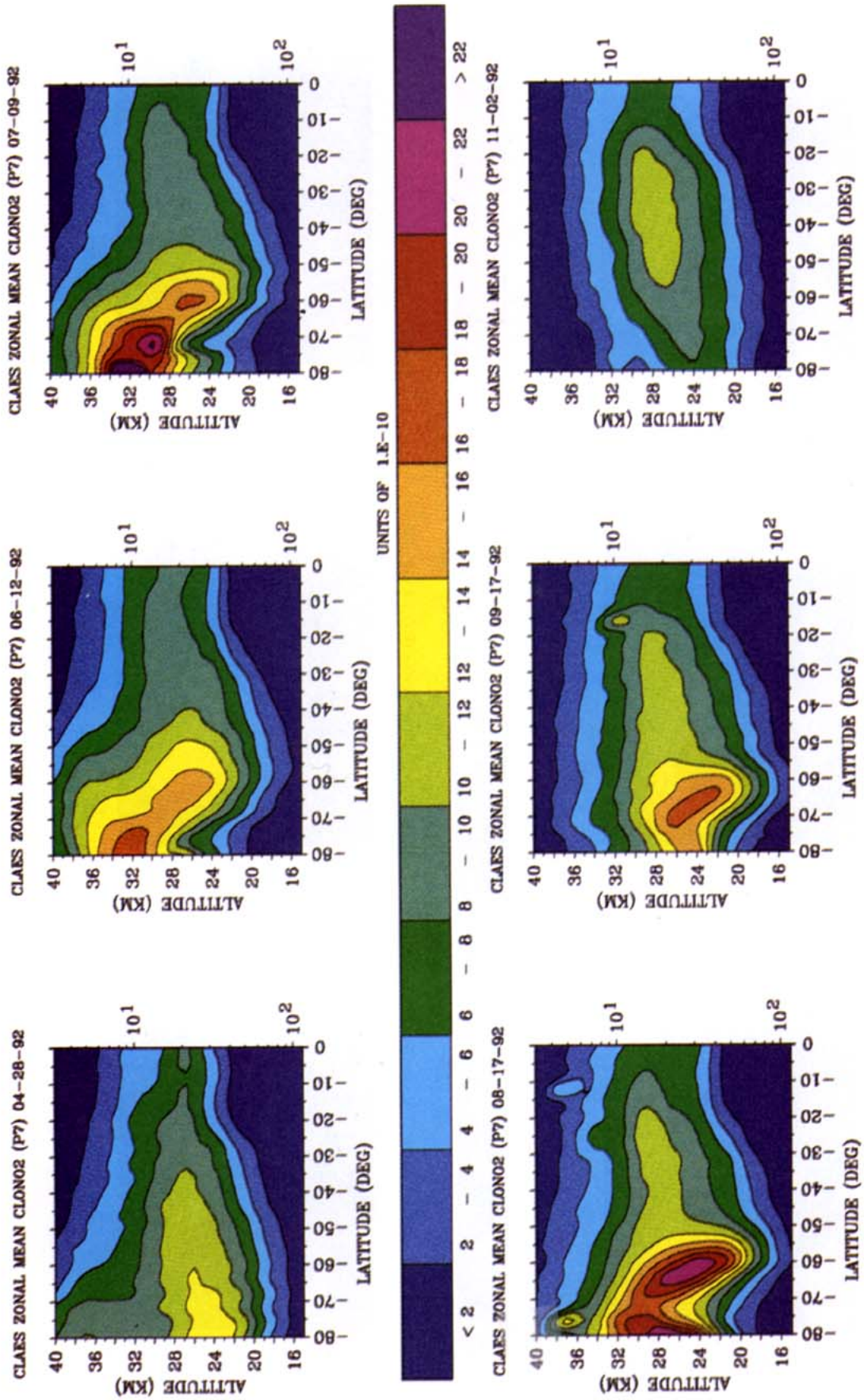

FIG. 7. Zonal-mean stratospheric altitude profiles of Southern Hemispheric $ClONO_2$ VMR (ppbv $\times$ 10) *as measured by* CLAES for individual days in April, June, July, August, September, and November 1992.

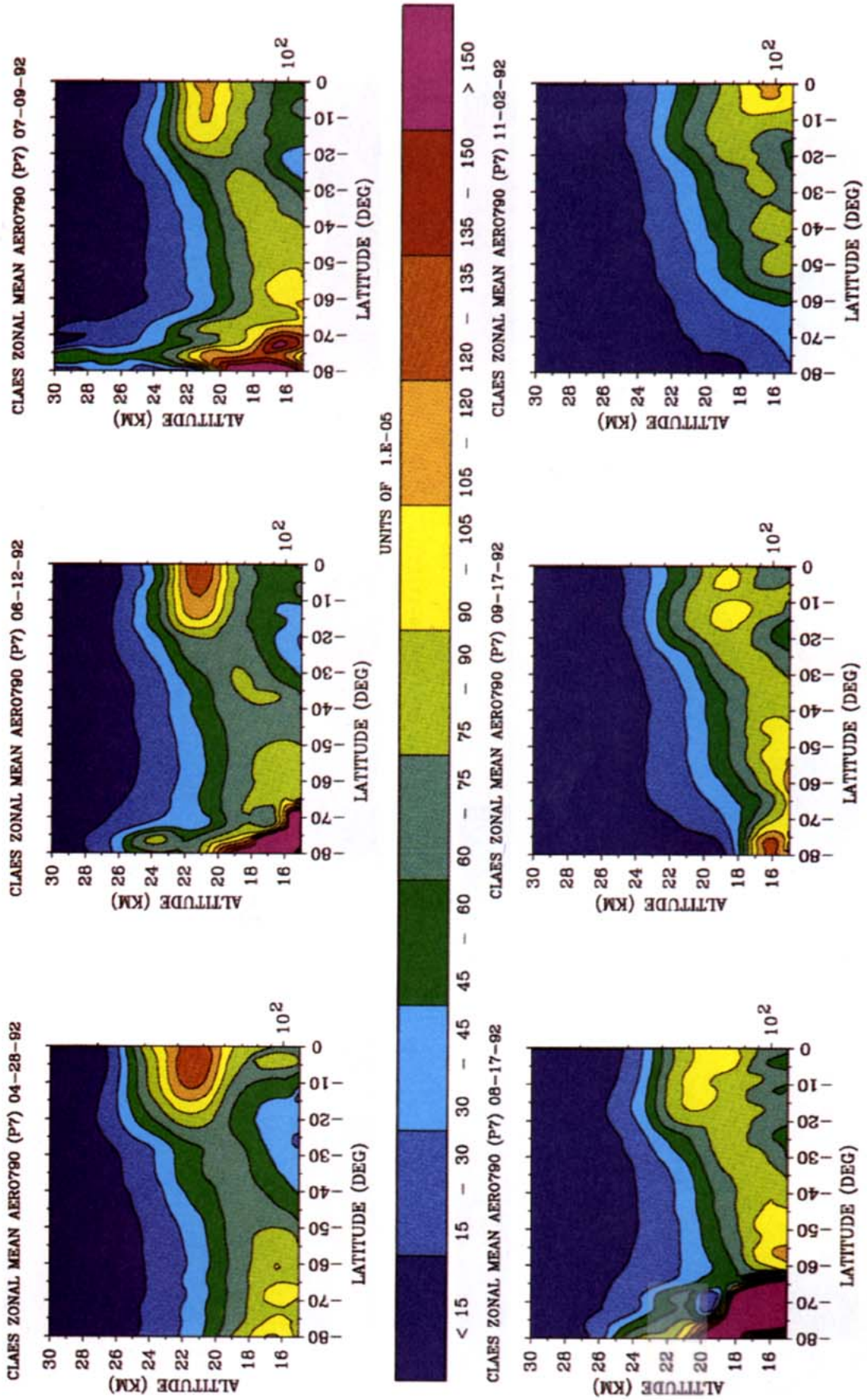

FIG. 8. Zonal-mean altitude profiles of Southern Hemispheric aerosol extinction coefficient (10^{-5} km^{-1}) as measured by CLAES for individual days in April, June, July, August, September, and November 1992.

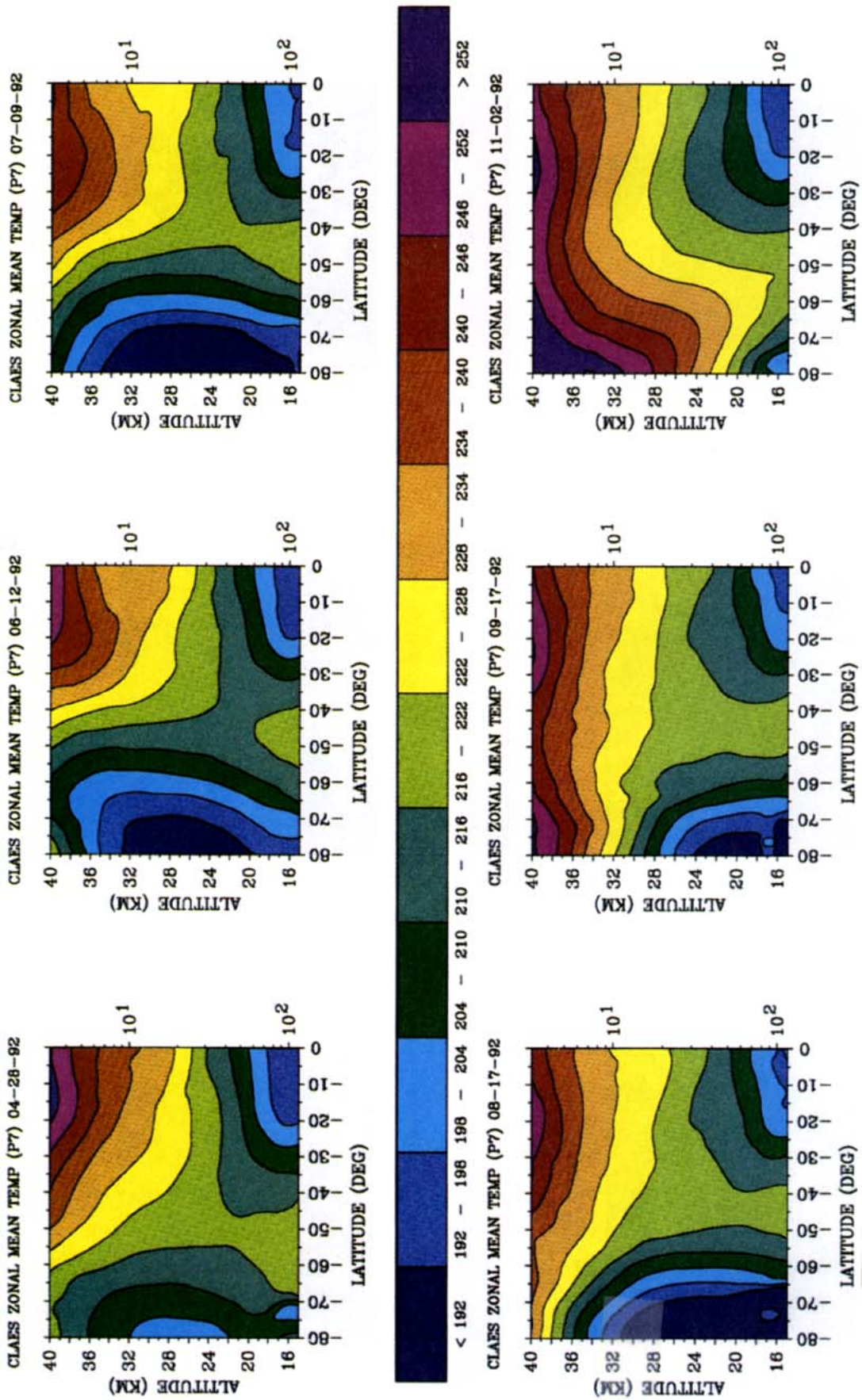

FIG. 9. Zonal-mean altitude profiles of Southern Hemispheric temperature (K) as measured by CLAES for individual days in April, June, July, August, September, and November 1992.

absence of any significant increase in HNO_3 in the vortex on 17 September might then suggest that PSCs, formed throughout the winter when it was cold enough and sequestering HNO_3, had largely sedimented to lower altitudes and were not available to resupply gaseous HNO_3 through evaporation in the spring. The LLNL model (Fig. 3b) in fact shows continued low levels of HNO_3 at 21 km near the South Pole into mid-October, well after temperatures have risen above the NAT formation level, consistent with removal of HNO_3 through PSC sedimentation. By early in the last CLAES southern look (2 November) the HNO_3 fields as seen in Fig. 6 have a much more uniform latitudinal appearance from midlatitudes to the South Pole, although values remain low near the pole, in comparison to 28 April, for example. On this day very low aerosol extinction coefficients are seen poleward of about 60°S at all stratospheric altitudes.

The somewhat elevated aerosol extinction values seen in the 28 April data from about 65° to 80°S are most likely sulfate aerosol, rather than PSCs. CLAES-measured zonal-mean temperatures in this region are all in excess of 204 K, almost certainly too warm to form type I PSCs for reasonable amounts of HNO_3 and H_2O. On the other hand, the Pinatubo sulfate layer was observed to have reached 80°S by 11 November 1991 (Lambert et al. 1993), and the CLAES data for April 28 show a "bridge" of aerosol extending from the tropical maximum of the volcanic layer and descending toward the pole. One cause of the increase in the extinction of this transported sulfate aerosol from 60° to 80°S at the lower altitudes is likely to be water uptake on the aerosol as temperatures drop in the austral fall (Steele and Hamill 1981).

b. *$ClONO_2$: Zonal-mean altitude profiles—Southern Hemisphere*

Zonal means for $ClONO_2$ for the same 6 days as for HNO_3 are shown in Fig. 7. Unlike HNO_3, which is seen to be highly eroded during this period close to the pole throughout the lower and middle stratosphere, the $ClONO_2$ depletion region is primarily confined to the lower stratosphere in the region of most intense PSC activity. Apart from this "erosion" region below about 24 km, $ClONO_2$ peak values are seen to increase substantially from 60° to 80°S latitudes between 12 June and 17 August. This may be because of the decreasing photolysis of $ClONO_2$ during the polar night winter and decreasing temperatures, which favor the three-body conversion of ClO and NO_2 to $ClONO_2$. Peak values are seen to have diminished by 17 September, close to the equinox. By 2 November, the lower-stratosphere erosion feature near the pole has essentially disappeared, and the overall VMR has diminished substantially toward high latitudes.

The geographical structure of both HNO_3 and $ClONO_2$ fields in the lower stratosphere is revealed in

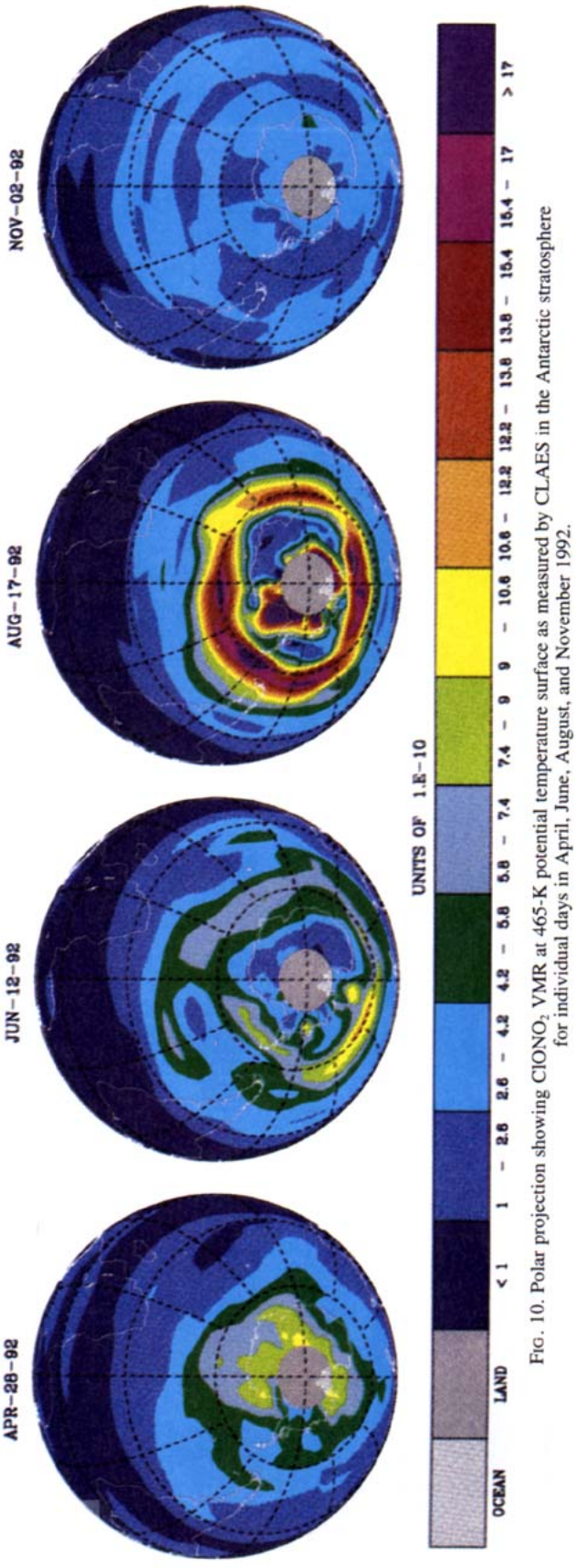

FIG. 10. Polar projection showing $ClONO_2$ VMR at 465-K potential temperature surface as measured by CLAES in the Antarctic stratosphere for individual days in April, June, August, and November 1992.

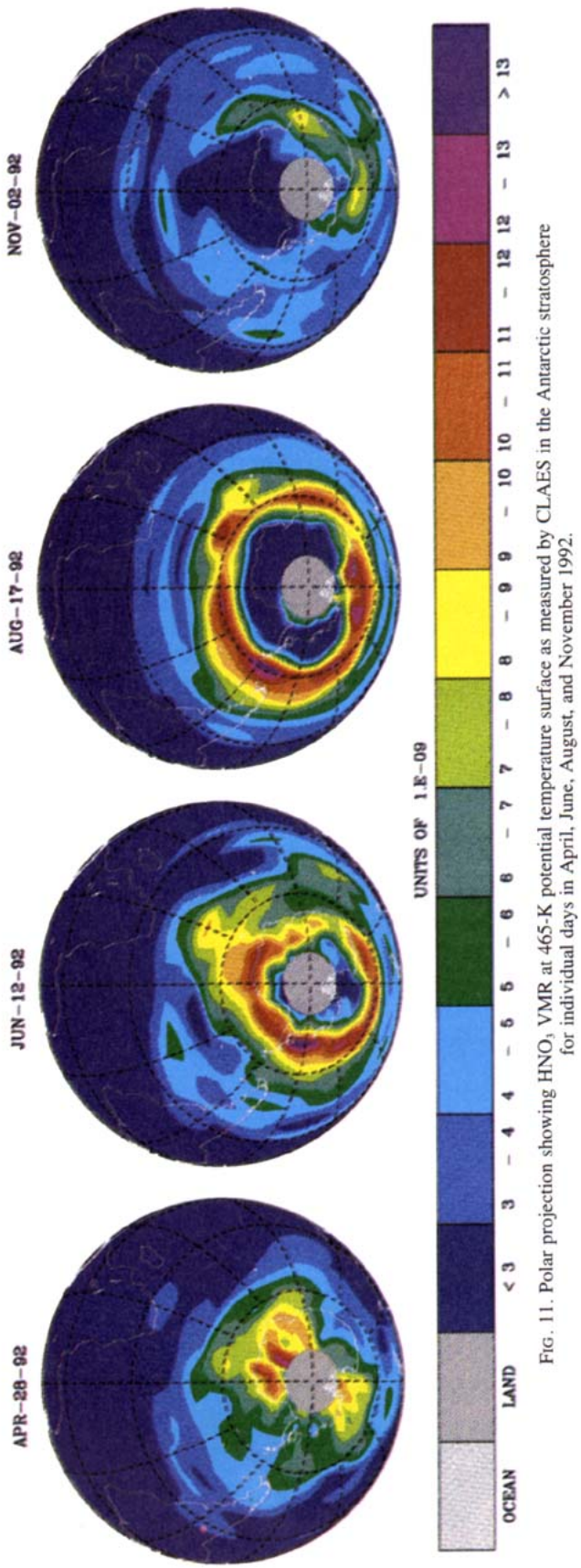

FIG. 11. Polar projection showing HNO_3 VMR at 465-K potential temperature surface as measured by CLAES in the Antarctic stratosphere for individual days in April, June, August, and November 1992.

Figs. 10 and 11 for four of the six days discussed in relation to Fig. 6. For comparison, Figs. 12 and 13 show temperature and aerosol extinction coefficient obtained by CLAES for the same days. These are polar orthographic projections of 24 hours of data gridded at 465-K potential temperature surface, which corresponds approximately to 70 mb (about 18 km) outside the cold vortex, and 46 mb (about 21 km) inside the vortex. For the April days shown, high-latitude temperatures are still well above 195 K. Aerosol extinction levels are generally characteristic of midlatitude values—that is, the very high levels associated with the presence of PSCs are not yet seen and both HNO_3 and $ClONO_2$ show increasing values poleward of about 60°S. By 12 June, temperatures have dropped below 192 K in an asymmetrical band around the pole and below 189 K in an area west of the Antarctic continent. High extinction coefficients are now seen within the cold areas, indicating the presence of PSCs. Both the HNO_3 and $ClONO_2$ fields have assumed a structure characterized by a band or collar region of high values outside the vortex edge, as defined here by the steepest temperature gradients; then both constituents drop off steeply to low values inside the vortex. This structure is even more pronounced for 17 August, for which the cold temperature regime has expanded considerably and the PSCs are seen extending to 60°S (Fig. 13). This structure has been observed previously by aircraft (Toon et al. 1989) in column measurements in the Antarctic spring. Again the constituent fields show their steepest gradients to low values largely coincident with the steepest temperature gradients and follow the asymmetric shape of the vortex edge.

A line plot at 80°E longitude through the collar region is shown in Fig. 14 for 17 August. The coincidence of HNO_3 and $ClONO_2$ with the vortex edge is clearly illustrated by comparison with CLAES temperature, the tracer CH_4, and potential vorticity. The initial steep gradient in tracers (at about 60°S for this day and longitude) indicating a region of sharp descent in the polar air has been referred to as the dynamical edge of the vortex (Schoeberl and Hartmann 1991). Figure 14 shows that both $ClONO_2$ and HNO_3 drop off steeply at the dynamical edge and are significantly depleted by about 70°S. The chemically perturbed region, or CPR, defined as the region where ClO is observed to increase steeply, typically occurs inside this dynamical edge (Schoeberl and Hartmann 1991; Proffitt et al. 1989). The MLS instrument on *UARS*, for example, for this same day (Waters et al. 1993a) shows ClO peaking along the 80°E longitude between about 65° and 70°S, in the region of low CLAES HNO_3 and $ClONO_2$. The steep descent of air inside the vortex as implied by the CH_4 data in Fig. 14 would result, in the absence of any removal mechanisms, in an increase in lower-stratospheric HNO_3 and $ClONO_2$. The observation that $ClONO_2$ and HNO_3 decrease so dramatically in the winter inside the vortex is an indication of the effi-

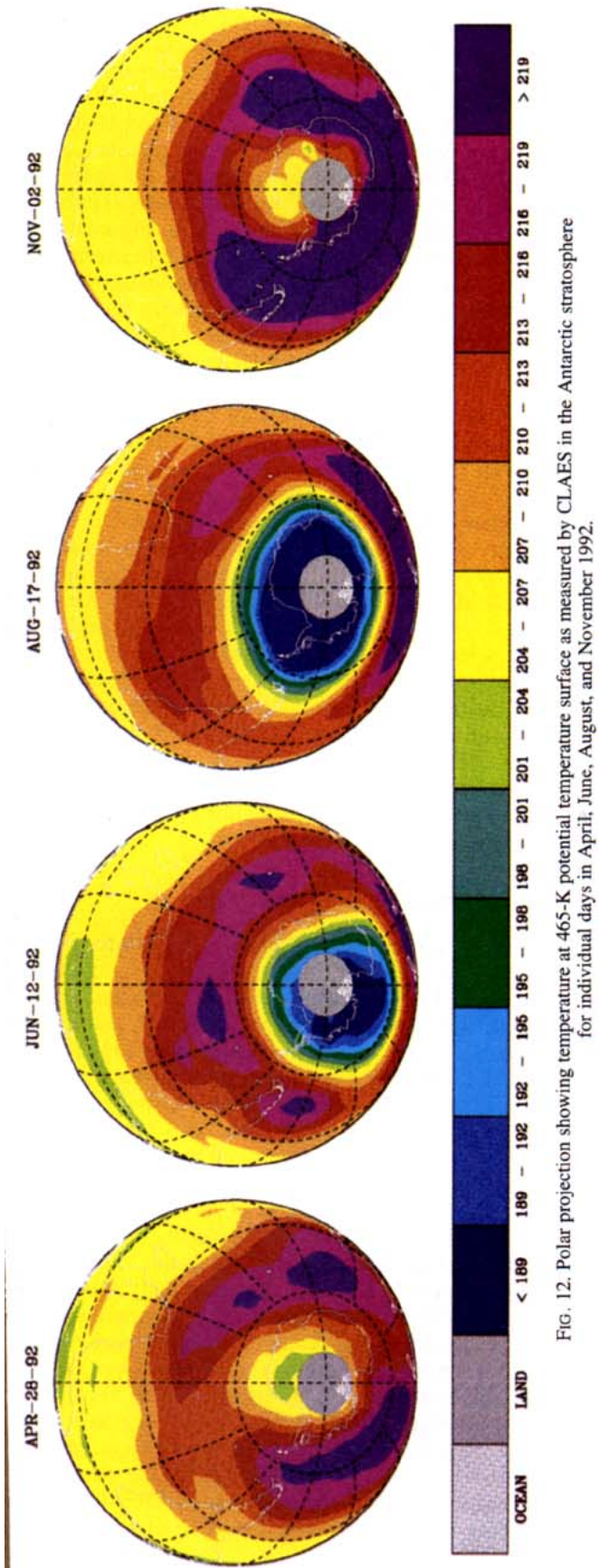

FIG. 12. Polar projection showing temperature at 465-K potential temperature surface as measured by CLAES in the Antarctic stratosphere for individual days in April, June, August, and November 1992.

ciency of removal of HNO_3 through PSC formation and of the heterogeneous conversion of $ClONO_2$ on the PSCs. The observation of high levels of ClO in the region of depleted $ClONO_2$, as noted above, is consistent with the heterogeneous production of active chlorine from the $ClONO_2$ (and HCl) reservoirs.

Figure 12 shows that on 2 November temperatures have risen well above 195 K, and aerosol extinction is very low poleward of 60°S. The high collar values have essentially dissipated for both $ClONO_2$ and HNO_3, but mixing ratios remain generally low over Antarctica (Figs. 10 and 11).

4. High-latitude observations of $ClONO_2$, HNO_3, and aerosol in the Northern Hemisphere winter/spring

Figures 15, 16, and 17 show polar stereographic projections, respectively, of CLAES temperature, aerosol extinction, and NMC PV for individual days between 28 October 1992 and 15 March 1993. For the 28 October and 3 December dates, the vortex temperatures were generally at or above 195 K. On 15 February a large area with temperature in the range 192 to 195 K had developed, and on 22 February there were regions inside the vortex with temperatures below 189 K (mainly over eastern Greenland, or between Greenland and Scandinavia). By 28 February, the vortex temperature had risen above 195 K, and it stayed at or above this level for the rest of the spring period. In comparison with the 1992 South Polar winter vortex, the 1992/93 northern vortex is seen to be much less symmetrically shaped and positioned with respect to the pole. It is much more variable in size and position and it does not maintain temperatures below 195 K for the same lengths of time or over the same geographical extent. It is clear from this behavior that a zonal-mean analysis would be much less useful for northern high-latitude winter conditions than for the Southern Hemisphere. We will present here only latitude/longitude cross sections to illustrate the behavior of the aerosol and gas species.

a. Aerosol

Extinction due to the Pinatubo sulfate aerosol, which is most evident for latitudes equatorward of about 60°N at the beginning of the five-month period shown in Fig. 16, is seen to decrease steadily throughout the period as the volcanic cloud dissipates. Aerosol extinction is in general noticeably lower inside the vortex than outside, especially for the colder periods between 3 December and 22 February, except for the localized regions on 15 February, and more distinctly on 22 February where high extinction levels are seen. The observed development of an aerosol extinction gradient at the vortex edge and low values inside the vortex have been related to subsidence (Kent et al. 1984). We per-

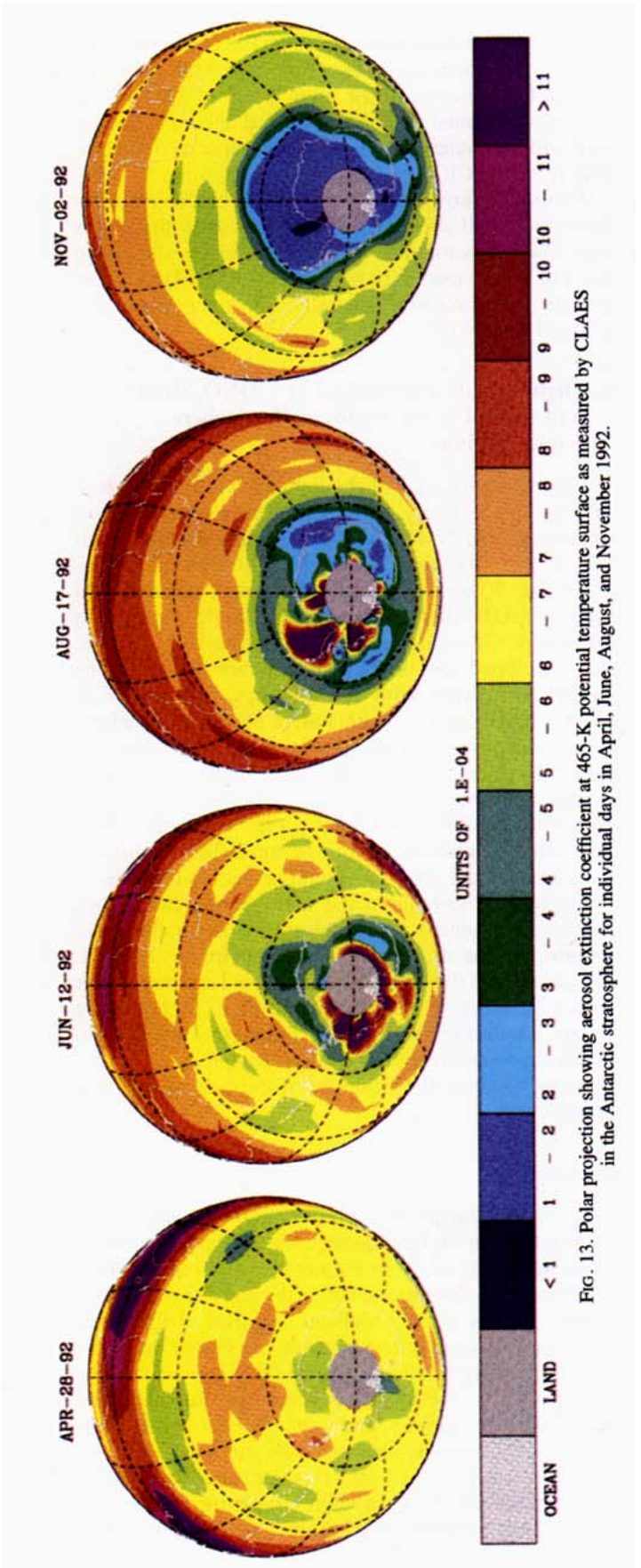

FIG. 13. Polar projection showing aerosol extinction coefficient at 465-K potential temperature surface as measured by CLAES in the Antarctic stratosphere for individual days in April, June, August, and November 1992.

formed a similar (approximate) NAT formation temperature calculation to that discussed previously (section 2c), for the three days 3 January, 15 February, and 22 February when vortex temperatures below 195 K were most widespread. The CLAES-retrieved HNO_3 VMRs shown in Fig. 18 were used in this calculation, along with H_2O mixing ratios in the range 4 to 5 ppmv, to yield a value for the NAT formation temperature between 194 and 195 K for all three days. Figure 16 shows no evidence of PSC formation inside the vortex on 3 January although temperatures appear close to or below 195 K. Since the estimated NAT formation temperature for this case is so close to the retrieved temperature, the nonappearance of PSC activity may simply be due to few degrees kelvin systematic temperature error. Alternatively, the lack of cloud formation may be the result of supersaturation of HNO_3 vapor with respect to NAT formation as has been observed previously in the Arctic (Kawa et al. 1992b). There is better evidence for PSC formation inside the vortex on 15 February. The peak extinction values lying just poleward of 60°N are substantially higher than the surrounding fields and are roughly aligned with the coldest patches ($T < 192$ K) inside the vortex. Finally, on 22 February, which has the coldest overall vortex temperature of any of the days shown, there is very clear evidence for a strong PSC event aligned with the coldest region between Greenland and northern Europe. Given that the vortex temperatures in this region are of the order of 5–6 K colder than the estimated NAT formation temperature, it seems likely that this intense extinction feature is due to type I PSCs.

b. HNO_3: Northern Hemisphere

HNO_3 polar projections are shown in Fig. 18 for the same eight days listed for Figs. 13–15. In general, the highest levels of HNO_3 in the Northern Hemisphere are seen inside the vortex throughout this period, and the HNO_3 fields are well correlated with PV (Fig. 17). The HNO_3 VMR inside the vortex is seen to increase substantially between 25 October and 3 December and reaches levels in excess of 13 ppbv on 3 January. It then decreases in February and March but is still present at a level of 7–8 ppbv on 14 March. There is an indication of localized depletion of HNO_3 inside the vortex on 22 February in the vicinity of the PSC seen in Fig. 16. Lower HNO_3 values overlap the PSC, but the deepest region of HNO_3 depletion actually appears somewhat east of the cloud center. This apparent eastward displacement of the center of depletion region is also seen in the $ClONO_2$ fields for 22 February (Fig. 19) and will be the subject of further analysis, including the consideration of wind fields for the region.

In summary, HNO_3 is seen in relatively large concentrations inside the vortex throughout the period, similar to observations of the 1989 Arctic vortex (Toon et al. 1992). There is no clear evidence of strong or

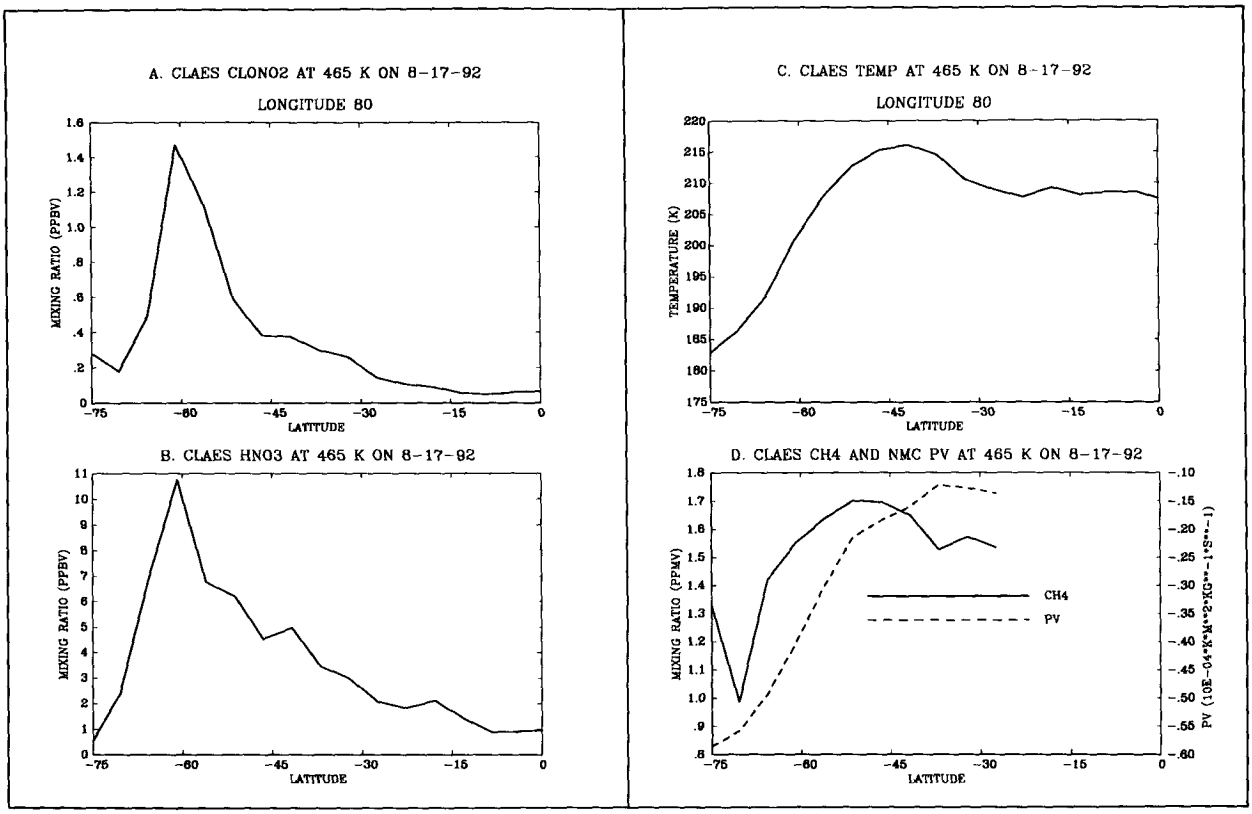

FIG. 14. (a) Cross section at 80°E through the $ClONO_2$ fields at 46 mb in the Antarctic stratosphere for the 17 August data shown in Fig. 10. (b) Same as (a) but for HNO_3 from Fig. 11. (c) Same as (a) but for CLAES temperature from Fig. 12. (d) Same as (a) but for CLAES CH_4 and NMC-derived potential vorticity.

sustained depletion regions associated with cold temperatures for the eight days shown, although there is an indication of localized depletion on 22 February, the coldest vortex day examined. Compared to the low HNO_3 values seen inside the South Polar vortex in winter and spring months at this same 465-K level, it would appear that the Arctic winter stratosphere is not being significantly denitrified.

c. *$ClONO_2$: Northern Hemisphere*

$ClONO_2$ for the same Northern Hemisphere days is shown in Fig. 19. The most notable feature of the $ClONO_2$ fields for the period shown is the rapid buildup of the VMR inside the vortex from 15 February through 7 March, with the highest values inside the warmer vortices on 7 March and 14 March. On 7 March VMRs in excess of 2.1 ppbv are seen throughout the vortex, and a week later on 14 March levels in excess of 2 ppbv are still maintained in large areas. The $ClONO_2$ fields are highly correlated with PV throughout the period shown, but particularly for the February and March days. As noted previously there is an indication of localized $ClONO_2$ depletion inside the vortex on 22 February, collocated with the lowest values of HNO_3 in that region.

The high levels of $ClONO_2$ seen in the Arctic spring represent a large fraction of the total inorganic chlorine in the lower stratosphere. Combined with the presence of substantial amounts of HNO_3, it would appear that the repartitioning of active chlorine in the spring following its production in the winter by heterogeneous processes highly favors the path through the reaction of ClO and NO_2 to form $ClONO_2$. This process has been discussed in relation to measurements of Arctic ClO and HCl in 1992 during the AASE2 campaign (Webster et al. 1993), but without the direct and simultaneous measurement of $ClONO_2$, HNO_3, PSCs, and temperatures throughout the polar night and recovery period, as provided by these CLAES data. These data clearly show the buildup of $ClONO_2$ during February and March 1993 to values considerably higher than the initial amount, as suggested by Webster et al. for the 1992 Arctic vortex.

5. Summary and conclusions

a. *Southern Hemisphere*

For periods between 12 June and 1 September 1992 at latitudes poleward of about 65°S, when temperatures were below the estimated 190–194-K type I PSC for-

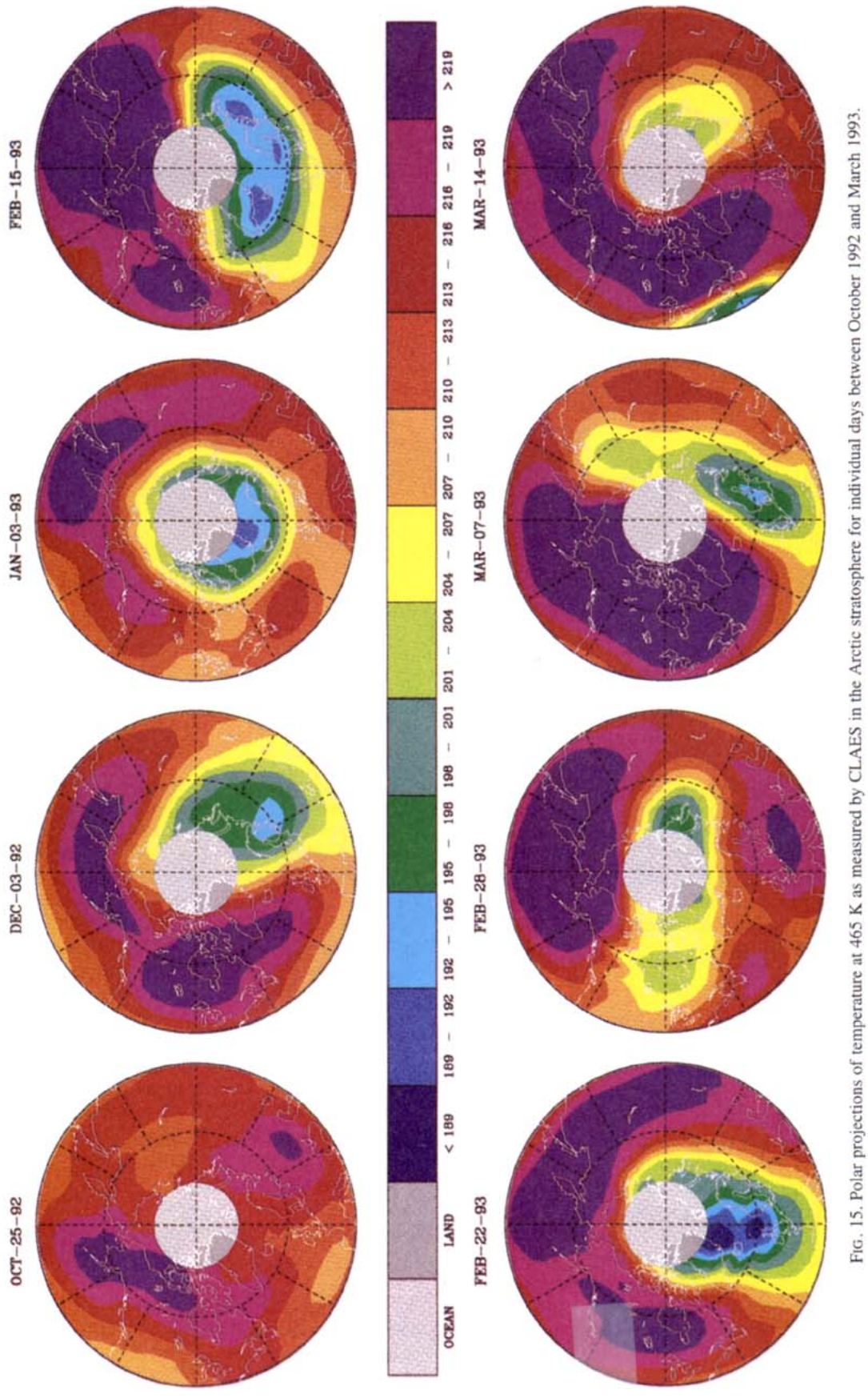

FIG. 15. Polar projections of temperature at 465 K as measured by CLAES in the Arctic stratosphere for individual days between October 1992 and March 1993.

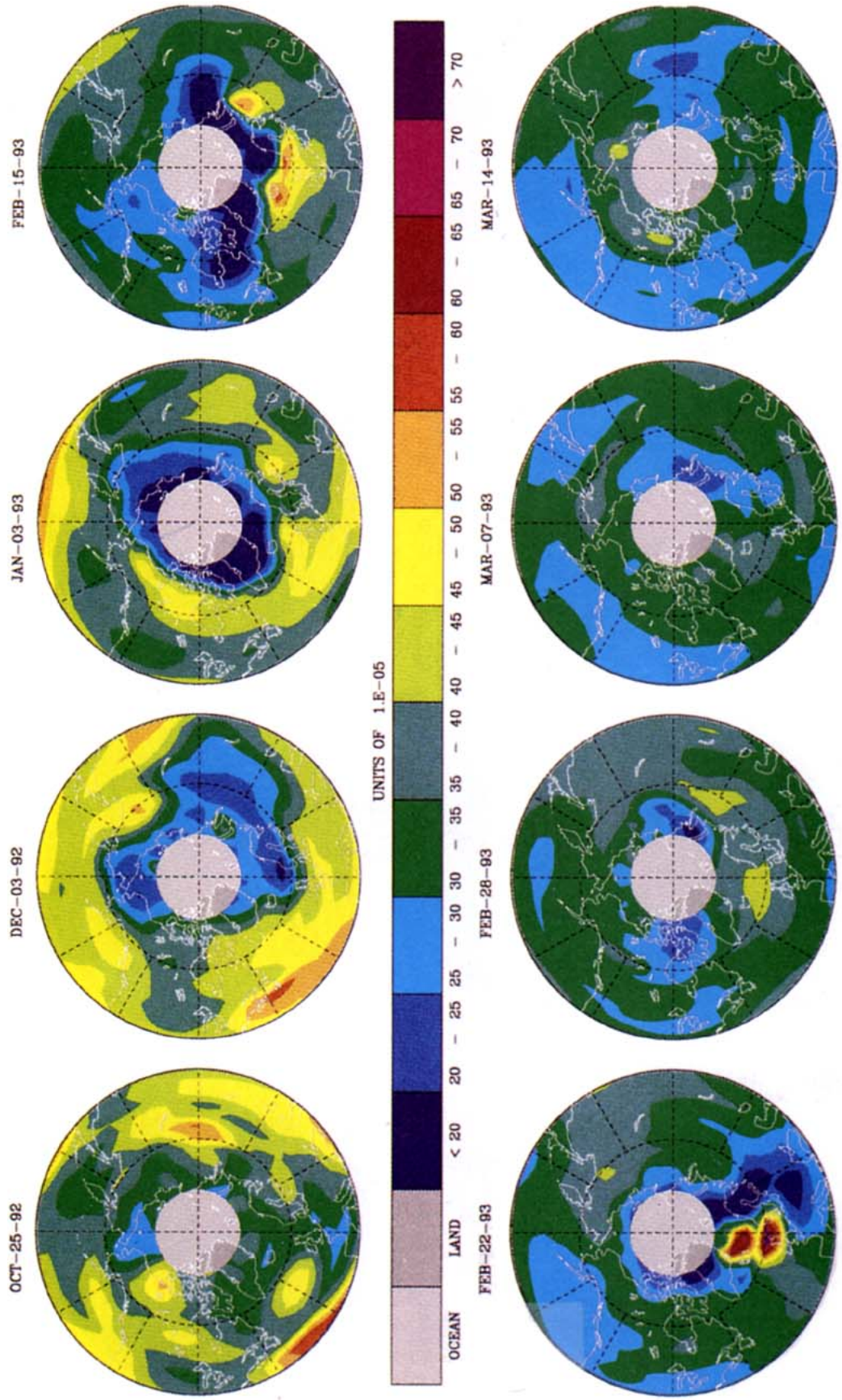

FIG. 16. Polar projections of aerosol extinction coefficients as measured by CLAES in the Arctic stratosphere for individual days between October 1992 and March 1993.

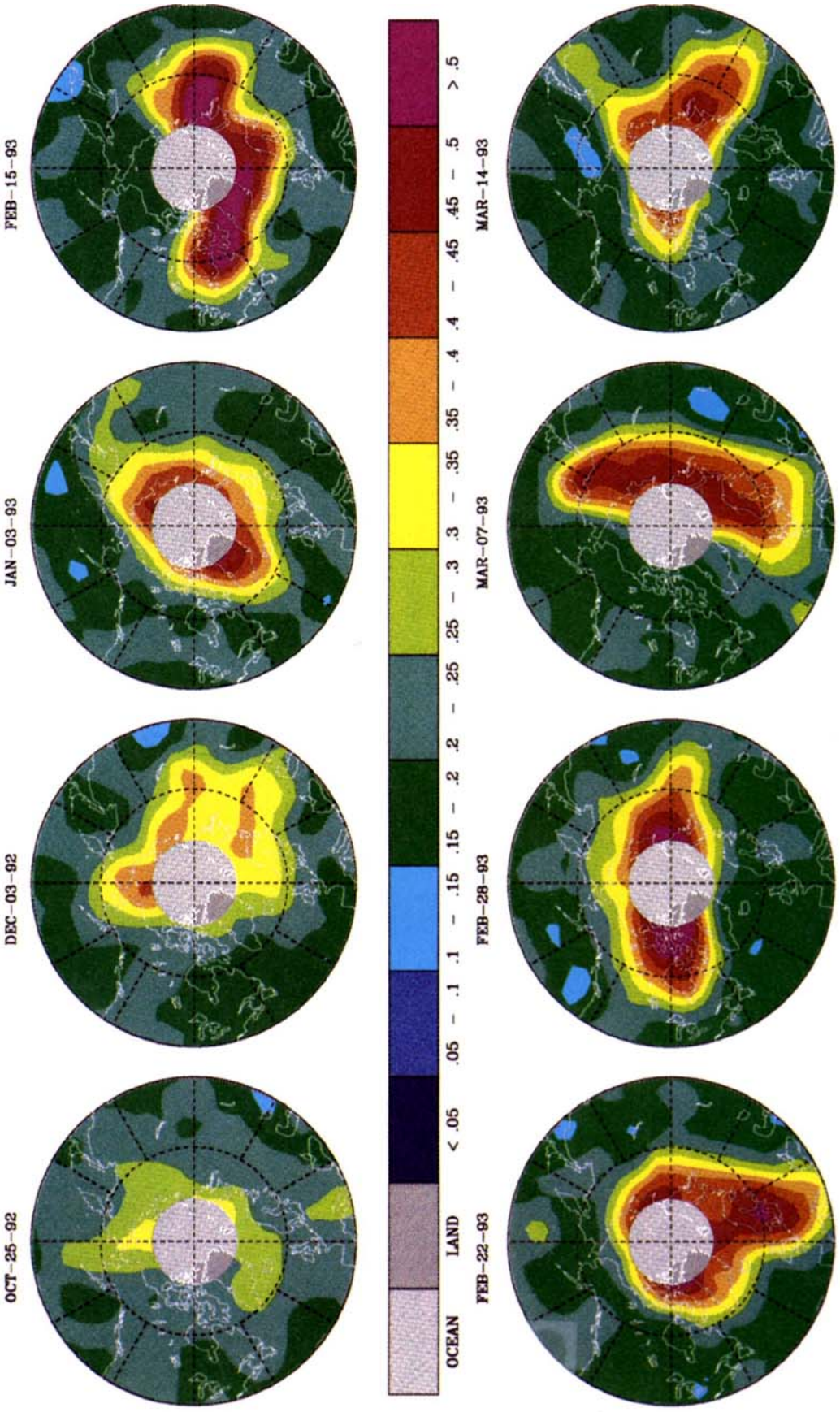

FIG. 17. Polar projections of NMC-derived potential vorticity in the Arctic stratosphere for individual days between October 1992 and March 1993.

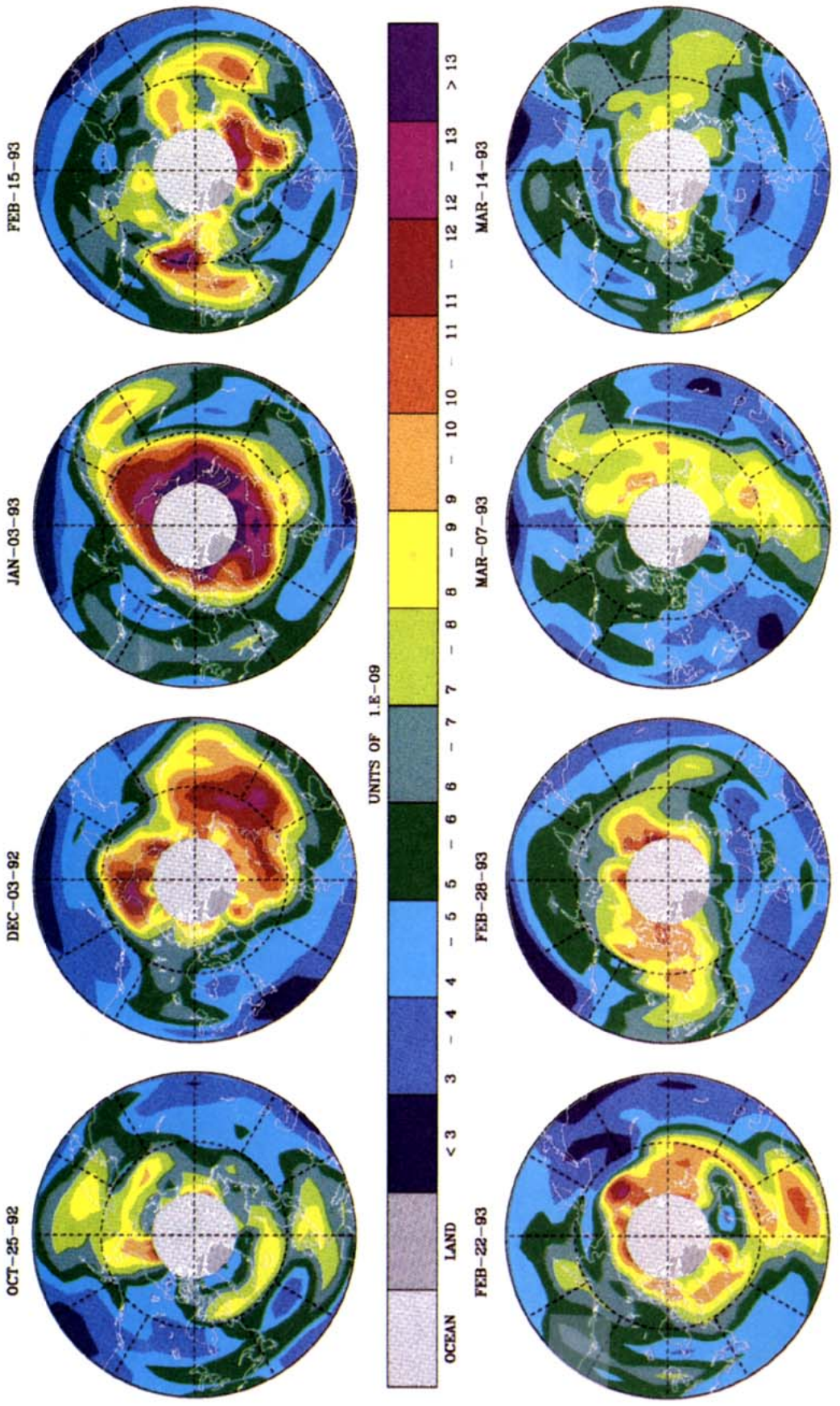

FIG. 18. Polar projections of HNO_3 VMR at 465 K as measured by CLAES in the Arctic stratosphere for individual days between October 1992 and March 1993.

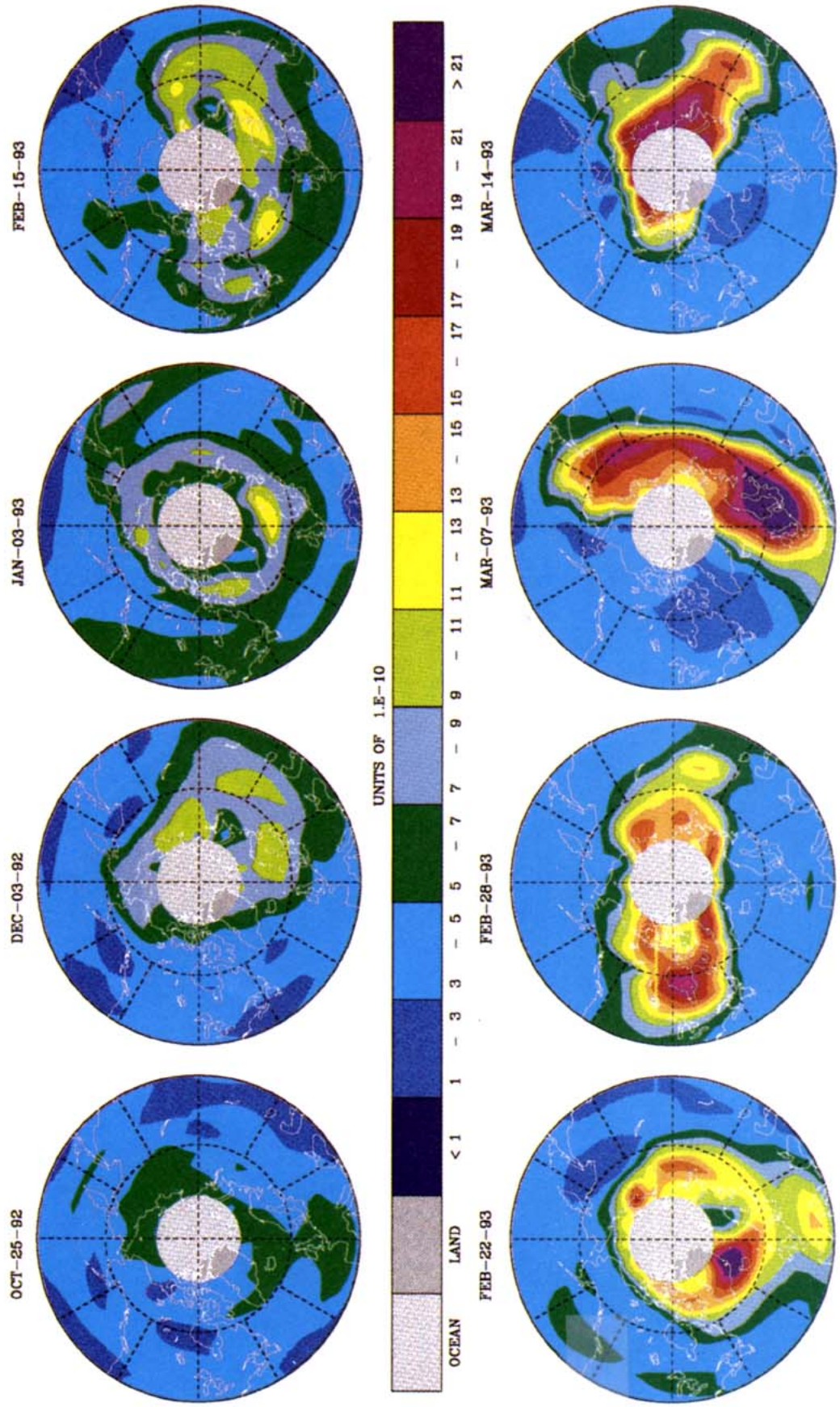

FIG. 19. Polar projections of $ClONO_2$ VMR at 465 K as measured by CLAES in the Arctic stratosphere for individual days between October 1992 and March 1993.

mation temperature throughout the lower stratosphere, CLAES observed high levels of PSCs coincident with highly depleted VMRs of both HNO_3 and $ClONO_2$. While the $ClONO_2$ was depleted at these latitudes mainly below about 23 km, HNO_3 was substantially depleted to altitudes as high as 30 km. Both gases developed enhanced collar regions near 60°S and very steep gradients as the levels dropped off toward the pole, closely correlated with similar gradients in the tracer CH_4 and with PV, defining the dynamical edge of the polar vortex. By 17 September, the incidence of PSCs had greatly diminished in the lower stratosphere, but both $ClONO_2$ and HNO_3 remained highly depleted. By 2 November, the time of the next CLAES look at the South Pole, the vortex had largely broken up, temperatures were well above 195 K, and quite low aerosol extinction was seen in the polar region. The collar structure in $ClONO_2$ and HNO_3 had greatly diminished and VMRs for both species had risen substantially in the previously depleted regions, although not to their prewinter levels.

The observation of high levels of PSCs in cold temperature regions inside the vortex coincident with low levels of HNO_3 and $ClONO_2$ is consistent with the removal of gaseous HNO_3 through the formation of NAT particles and the removal of $ClONO_2$ through heterogeneous reactions on the particle surfaces. The observation of high levels of ClO inside the cold vortex by the *UARS* MLS instrument during the same periods of time that CLAES observed depleted $ClONO_2$ is strong evidence that these heterogeneous reactions convert inactive chlorine in the $ClONO_2$ and HCl reservoirs to free chlorine. HNO_3, a product of these reactions, must stay sequestered on the particle surfaces to maintain the low levels of gaseous HNO_3 observed. The copious amounts of $ClONO_2$ in the collar region near the dynamical edge of the cold vortex indicate that ClO is being produced heterogeneously in this region but is rapidly converted to $ClONO_2$ by reaction with NO_2, where the NO_2 is formed from photolysis of HNO_3. Deeper inside the vortex, the HNO_3 is too depleted to provide NO_2 for the suppression of ClO. The rapid depletion of O_3 in September/October through catalytic reactions involving ClO requires that these low levels of HNO_3 be maintained during this period—that is, evaporating PSCs cannot resupply gaseous HNO_3 and therefore must have been removed prior to the onset of rapid ozone loss. The lower stratosphere therefore appears to be substantially denitrified in the southern vortex through sedimentation of NAT particles.

b. *Northern Hemisphere*

In the Northern Hemisphere winter of 1992/93 many fewer PSCs were observed in the lower stratosphere inside the polar vortex, consistent with the generally shorter periods, and in more localized regions where temperatures dropped below the estimated 194–195 K type I PSC formation temperature. While both HNO_3 and $ClONO_2$ showed regions of localized depletion in the vicinity of intense PSCs on one of the coldest days examined, in general they both maintained substantial levels inside the vortex throughout the winter/spring period. Following 28 February, when vortex temperatures rose above 195 K and stayed at higher levels for the rest of the spring, $ClONO_2$ was observed in large quantities (>2.1 ppbv at 465-K potential temperature) inside the vortex and was highly correlated with the vortex boundary as defined by both temperature and PV gradients.

The CLAES observations of PSCs associated with localized depletion of HNO_3 and $ClONO_2$, and the observation of enhanced levels of ClO in the 1993 Arctic winter vortex (Waters et al. 1993b), are strong evidence that similar heterogeneous processing of lower-stratospheric air, which chemically perturbs the Antarctic winter vortex, is also occurring in the Arctic. However, the persistence of relatively high levels of HNO_3 inside the Arctic spring vortex, compared with the continuing low levels seen in the Antarctic spring vortex, indicates a much lower level of denitrification in the Arctic. These high levels of HNO_3 are thought to lead to the production of sufficient amounts of NO_2 to suppress ClO through the formation of $ClONO_2$ (Webster et al. 1993). The CLAES observation of substantially enhanced levels of $ClONO_2$ in the spring supports this theory. With reduced levels of ClO, the ClO-driven O_3 catalytic loss process responsible for the Antarctic spring ozone hole would be much less efficient in producing substantial O_3 losses in the Arctic spring stratosphere.

Acknowledgments. We thank Frank Zele at Lockheed for his contributions to the production of the figures presented in this paper and Gloria Manney at JPL for providing us with potential vorticity data and our colleagues at NCAR for their contributions to CLAES data validation and analysis. We also acknowledge the very helpful comments of the reviewers of this paper. This work was performed under NASA Contract NAS5-27752, and DOE contract W-7405-ENG-48.

REFERENCES

Deshler, T., B. J. Johnson, and W. R. Rozier, 1994: Changes in the character of polar stratospheric clouds over Antarctica in 1992 due to the Pinatubo volcanic aerosol. *Geophys. Res. Lett.*, **21**, 273–276.

Fahey, D. W., K. K. Kelly, G. V. Ferry, L. R. Poole, J. C. Wilson, D. M. Murphy, M. Loewenstein, and K. R. Chan, 1989: In situ measurements of total reactive nitrogen, total water and aerosol in a polar stratospheric cloud in the Antarctic. *J. Geophys. Res.*, **94**, 11 299–11 315.

——, S. Solomon, S. R. Kawa, M. Loewenstein, J. R. Podolske, S. E. Straham, and K. R. Chan, 1990: A diagnostic for denitrification in the winter polar stratospheres. *Nature*, **345**, 698–702.

Gille, J. C., J. M. Russell III, P. L. Bailey, E. E. Remsberg, L. L. Gordley, W. F. J. Evans, H. Fischer, B. W. Gandrud, A. Girard,

J. E. Harries, and S. A. Beck, 1984: Accuracy and precision of the nitric acid concentrations determined by the limb infrared monitor of the stratosphere. *J. Geophys. Res.*, **89,** 5179.

Hanson, D., and K. Mauersberger, 1988: Laboratory studies of the nitric acid trihydrate: Implications for the south polar stratosphere. *Geophys. Res. Lett.*, **15,** 855–858.

Kawa, S. R., D. W. Fahey, L. E. Heidt, W. H. Pollock, S. Solomon, D. E. Anderson, M. Loewenstein, M. H. Proffitt, J. J. Margitan, and K. R. Chan, 1992a: Photochemical partitioning of the reactive nitrogen and chlorine reservoirs in the high latitude stratosphere. *J. Geophys. Res.*, **97,** 7905–7923.

——, ——, K. K. Kelly, J. E. Dye, D. Baumgardner, B. W. Gandrud, M. Loewenstein, G. V. Ferry, and K. R. Chan, 1992b: The arctic polar stratospheric cloud aerosol: Aircraft measurements of reactive nitrogen, total water and particles. *J. Geophys. Res.*, **94,** 7925–7938.

Kent, G. S., C. R. Trepte, U. O. Farrukh, and M. P. McCormick, 1984: Variation in the stratospheric aerosol associated with the north cyclonic polar vortex as measured by the SAM II satellite sensor. *J. Atmos. Sci.*, **47,** 1536–1551.

Kumer, J. B., J. L. Mergenthaler, and A. E. Roche, 1993: CLAES CH_4, N_2O, and CCl_2F_2 (F 12) global data. *Geophys. Res. Lett.*, **20,** 1239–1242.

Lambert, A., R. G. Grainger, J. J. Remedios, C. D. Rodgers, M. Corney, and F. W. Taylor, 1993: Measurement of the evolution of the Mt. Pinatubo aerosol cloud by ISAMS. *Geophys. Res. Lett.*, **20,** 1287–1290.

Manney, G. L., and R. W. Zurek, 1993: Interhemispheric comparison of the development of the stratospheric polar vortex during fall: A 3-dimensional perspective for 1991–1992. *Geophys. Res. Lett.*, **20,** 1275–1278.

Marti, J., and K. Mauersberger, 1991: HCl dissolved in solid mixtures of nitric acid and ice: Implications for the polar stratosphere. *Geophys. Res. Lett.*, **18,** 1861–1864.

Mergenthaler, J. L., J. B. Kumer, and A. E. Roche, 1993: CLAES south-looking aerosol observations for 1992. *Geophys. Res. Lett.*, **20,** 1295–1298.

Molina, M. J., R. Zhang, P. J. Woolridge, J. R. McMahon, J. E. Kim, H. Y. Chang, and K. D. Beyer, 1993: Physical chemistry of the $H_2SO_4/HNO_3/H_2O$ system: Implications for polar stratospheric clouds. *Nature,* **261,** 1418–1423.

Patten, K. O., P. S. Connell, D. E. Kinnison, D. J. Wuebbles, T. G. Slanger, and L. Froidevaux, 1994: Effect of vibrationally excited oxygen on ozone production in the stratosphere. *J. Geophys. Res.*, **99,** 1211–1223.

Proffitt, J. A., Powell, A. F. Tuck, D. W. Fahey, K. K. Kelley, A. J. Krueger, M. R. Schoeberl, B. L. Gary, J. J. Margitan, K. R. Chan, M. Loewenstein, and J. R. Podolske, 1989: A chemical definition of the boundary of the Antarctic ozone hole. *J. Geophys. Res.*, **94,** 11 437–11 448.

Reber, C. A., 1993: The upper atmosphere research satellite (UARS). *Geophys. Res. Lett.*, **20,** 1215–1218.

Roche, A. E., J. B. Kumer, and J. L. Mergenthaler, 1993a: CLAES observations of $ClONO_2$ and HNO_3 in the Antarctic stratosphere between June 15, and September 17, 1992. *Geophys. Res. Lett.*, **20,** 1223–1226.

——, ——, ——, G. A. Ely, W. G. Uplinger, J. F. Potter, T. C. James, and L. W. Sterritt, 1993b: The cryogenic limb array etalon spectrometer (CLAES) on UARS: Experiment description and performance. *J. Geophys. Res.*, **98,** 12 763–12 775.

Rodriguez, J. M., 1993: Probing stratospheric ozone. *Science,* **261,** 1128–1129.

Salawitch, R. J., and coauthors, 1993: Chemical loss in the Arctic polar vortex in the winter of 1991–1992. *Science,* **261,** 1146–1149.

Schoeberl, M. R., and D. L. Hartmann, 1991: The dynamics of the stratospheric polar vortex and its relation to springtime ozone depletions. *Science,* **251,** 46–52.

Solomon, S., 1990: Progress towards a quantitative understanding of Antarctic ozone depletion. *Nature,* **347,** 347–354.

Steele, H. M., and P. Hamill, 1981: Effects of temperature and humidity on the growth and optical properties of sulfuric acid–water droplets in the stratosphere. *J. Aerosol Sci.*, **12,** 517–528.

Toon, G. C., C. B. Farmer, L. L. Lowes, P. W. Schaper, J. F. Blavier, and R. H. Norton, 1989: Infrared aircraft measurements over Antarctica during September 1987. *J. Geophys. Res.*, **94,** 16 571–16 596.

——, ——, P. W. Schaper, L. L. Lowes, and R. H. Norton, 1992: Composition measurements of the 1989 Arctic winter stratosphere by infrared solar absorption spectroscopy. *J. Geophys. Res.*, **97,** 7939–7961.

Tuck, A. F., R. T. Watson, E. P. Condon, J. J. Margitan, and O. B. Toon, 1989: The planning and execution of ER-2 and DC-8 aircraft flights over Antarctica, August and September 1987. *J. Geophys. Res.*, **94,** 11 181–11 122.

Turco, R., A. Plumb, and E. Condon, 1990: The Airborne Arctic Stratosphere Expedition: Prologue. *Geophys. Res. Lett.*, **17,** 313–316.

von Clarmann, T., H. Fischer, F. Friedl-Vallon, A. Linden, H. Oelhaf, C. Piesch, M. Seefeldner, and W. Volker, 1993: Retrieval of stratospheric O_3, HNO_3, and $ClONO_2$ profiles from 1992 MIPAS-B limb emission spectra. *J. Geophys. Res.*, **98,** 20 495–20 506.

Waters, J. W., L. Froidevaux, G. L. Manney, W. G. Read, and L. S. Elson, 1993a: MLS observations of stratospheric ClO and O_3 in the 1992 Southern Hemisphere winter. *Geophys. Res. Lett.*, **20,** 1219–1222.

——, ——, W. G. Read, G. L. Manney, L. S. Elson, D. A. Flower, R. F. Jarnot, and R. S. Harwood, 1993b: Stratospheric ClO and ozone from the microwave limb sounder on the upper atmosphere research satellite. *Nature,* **362,** 597–602.

Webster, C. R., R. D. May, D. W. Toohey, L. M. Avallone, J. G. Anderson, P. Newman, L. Lait, M. R. Schoeberl, J. W. Elkins, and K. R. Chan, 1993: Chlorine chemistry on polar stratospheric cloud particles in the Arctic winter. *Science,* **261,** 1130–1134.

Wuebbles, D. J., D. E. Kinnison, K. E. Grant, and J. Lean, 1991: The effect of solar flux variations and trace gas emissions on recent trends in stratospheric ozone and temperature. *J. Geomag. Geoelectr.*, **43**(Suppl.), 709–718.